

1 **ANALYTICAL LOW-RANK COMPRESSION VIA PROXY POINT
2 SELECTION***

3 XIN YE[†], JIANLIN XIA[†], AND LEXING YING[‡]

4 **Abstract.** It has been known in potential theory that, for some kernels matrices corresponding
5 to well-separated point sets, fast analytical low-rank approximation can be achieved via the use of
6 proxy points. This proxy point method gives a surprisingly convenient way of explicitly writing out
7 approximate basis matrices for a kernel matrix. However, this elegant strategy is rarely known or
8 used in the numerical linear algebra community. It still needs clear algebraic understanding of the
9 theoretical background. Moreover, rigorous quantifications of the approximation errors and reliable
10 criteria for the selection of the proxy points are still missing. In this work, we use contour integration
11 to clearly justify the idea in terms of a class of important kernels. We further provide comprehensive
12 accuracy analysis for the analytical compression and show how to choose nearly optimal proxy points.
13 The analytical compression is then combined with fast rank-revealing factorizations to get compact
14 low-rank approximations and also to select certain representative points. We provide the error bounds
15 for the resulting overall low-rank approximation. This work thus gives a fast and reliable strategy
16 for compressing those kernel matrices. Furthermore, it provides an intuitive way of understanding
17 the proxy point method and bridges the gap between this useful analytical strategy and practical
18 low-rank approximations. Some numerical examples help to further illustrate the ideas.

19 **Key words.** kernel matrix, proxy point method, low-rank approximation, approximation error
20 analysis, hybrid compression, strong rank-revealing factorization

21 **AMS subject classifications.** 15A23, 65F30, 65F35

22 **1. Introduction.** In this paper, we focus on the low-rank approximation of some
23 kernel matrices: those generated by a smooth kernel function $\kappa(x, y)$ evaluated at two
24 well-separated sets of points $X = \{x_j\}_{j=1}^m$ and $Y = \{y_j\}_{j=1}^n$. We suppose $\kappa(x, y)$ is
25 analytic and a degenerate approximation as follows exists:

26 (1.1)
$$\kappa(x, y) \approx \sum_{j=1}^r \alpha_j \psi_j(x) \varphi_j(y),$$

27 where ψ_j 's and φ_j 's are appropriate basis functions and α_j 's are coefficients indepen-
28 dent of x and y . X and Y are well separated in the sense that the distance between
29 them is comparable to their diameters so that r in (1.1) is small. In this case, the
30 corresponding discretized kernel matrix as follows is numerically low rank:

31 (1.2)
$$K^{(X, Y)} \equiv (\kappa(x, y)_{x \in X, y \in Y}).$$

32 This type of problems frequently arises in a wide range of computations such as
33 numerical solutions of PDEs and integral equations, Gaussian processes, regression
34 with massive data, machine learning, and N -body problems. The low-rank approxi-
35 mation to $K^{(X, Y)}$ enables fast matrix-vector multiplications in methods such as the
36 fast multipole method (FMM) [15]. It can also be used to quickly compute matrix
37 factorization and inversion based on rank structures such as \mathcal{H} [19], \mathcal{H}^2 [2, 20], and

*Submitted for review.

Funding: The research of Jianlin Xia was supported in part by an NSF grant DMS-1819166.

[†]Department of Mathematics, Purdue University, West Lafayette, IN 47907 (ye83@purdue.edu, xiaj@purdue.edu).

[‡]Department of Mathematics and Institute for Computational and Mathematical Engineering, Stanford University, Stanford, CA 94305 (lexing@stanford.edu).

38 HSS [5, 48] forms. In fact, relevant low-rank approximations play a key role in rank-
 39 structured methods. The success of the so-called fast rank-structured direct solvers
 40 relies heavily on the quality and efficiency of low-rank approximations.

41 According to the Eckhart-Young Theorem [9], the best 2-norm low-rank approxi-
 42 mation is given by the truncated SVD, which is usually expensive to compute directly.
 43 More practical *algebraic compression* methods include rank-revealing factorizations
 44 (especially strong rank-revealing QR [18] and strong rank-revealing LU factorizations
 45 [37]), mosaic-skeleton approximations [44], interpolative decomposition [7], CUR de-
 46 compositions [29], etc. Some of these algebraic methods have a useful feature of
 47 *structure preservation* for $K^{(X,Y)}$: relevant resulting basis matrices can be subma-
 48 trices of the original matrix and are still discretizations of $\kappa(x, y)$ at some subsets.
 49 This is a very useful feature that can greatly accelerate some hierarchical rank struc-
 50 tured direct solvers [49, 27, 47]. However, these algebraic compression methods have
 51 $\mathcal{O}(rmn)$ complexity and are very costly for large-scale applications. The efficiency
 52 may be improved by randomized SVDs [21, 16, 31], which still cost $\mathcal{O}(rmn)$ flops.

53 Unlike fully algebraic compression, there are also various *analytical compression*
 54 methods that take advantage of degenerate approximations like in (1.1) to compute
 55 low-rank approximations. The degenerate approximations may be obtained by Taylor
 56 expansions, multipole expansions [15], spherical harmonic basis functions [42], Fourier
 57 transforms with Poisson's formula [1, 30], Laplace transforms with the Cauchy inte-
 58 gral formula [28], Chebyshev interpolations [10], etc. Various other polynomial basis
 59 functions may also be used [38].

60 These analytical approaches can quickly yield low-rank approximations to $K^{(X,Y)}$
 61 by explicitly producing approximate basis matrices. On the other hand, the resulting
 62 low-rank approximations are usually not structure preserving in the sense that the
 63 basis matrices are not directly related to $K^{(X,Y)}$. This is because the basis functions
 64 $\{\psi_j\}$ and $\{\varphi_j\}$ are generally different from $\kappa(x, y)$.

65 As a particular analytical compression method, the *proxy point method* has at-
 66 tracted a lot of interests in recent years. It is tailored for kernel matrices and is very
 67 attractive for different geometries of points [10, 32, 50, 52, 53]. While the methods
 68 vary from one to another, they all share the same basic idea and can be summarized
 69 in the surprisingly simple **Algorithm 1.1**, where the details are omitted and will be
 70 discussed later in later sections. Note that an explicit degenerate form (1.1) is not
 71 needed and the algorithm directly produces the matrix $K^{(X,Z)} \equiv (\kappa(x, y)_{x \in X, y \in Z})$ as
 72 an approximate column basis matrix in **Step 2**. This feature enables the extension of
 73 the ideas of the classical fast multipole method (FMM) [15] to more general situations,
 74 and examples include the recursive skeletonization [22, 32, 36] and kernel independent
 75 FMM [33, 52, 53]. The convenient extraction of an approximate column basis matrix
 76 is similar to some methods used for data analysis such as the Nyström method and
 77 the pseudo-input approximation [8, 13, 26, 40, 46]. (More discussions on this will be
 78 given in [section 5](#).)

Algorithm 1.1 Basic proxy point method for low-rank approximation

Input: $\kappa(x, y)$, X , Y

Output: Low-rank approximation $K^{(X,Y)} \approx AB$ ▷ Details in [sections 2 and 3](#)

- 1: Pick a *proxy surface* Γ and a set of *proxy points* $Z \subset \Gamma$
- 2: $A \leftarrow K^{(X,Z)}$
- 3: $B \leftarrow \Phi^{(Z,Y)}$ for a matrix $\Phi^{(Z,Y)}$ such that $K^{(X,Y)} \approx K^{(X,Z)}\Phi^{(Z,Y)}$

79 Notice that $|Z|$ is generally much smaller than $|Y|$ so that $K^{(X,Z)}$ has a much
 80 smaller column size than $K^{(X,Y)}$. It is then practical to apply reliable rank-revealing
 81 factorizations to $K^{(X,Z)}$ to extract a compact approximate column basis matrix for
 82 $K^{(X,Y)}$. This is a *hybrid (analytical/algebraic) compression* scheme, and the proxy
 83 point method helps to significantly reduce the compression cost.

84 The significance of the proxy point method can also be seen from another view-
 85 point: the selection of *representative points*. When a strong rank-revealing QR (SR-
 86 RQR) factorization or interpolative decomposition is applied to $K^{(X,Y)}$, an approx-
 87 imate row basis matrix can be constructed from selected rows of $K^{(X,Y)}$. Suppose
 88 those rows correspond to the points $\hat{X} \subset X$. Then \hat{X} can be considered as a subset
 89 of representative points. The analytical selection of \hat{X} is not a trivial task. However,
 90 with the use of the proxy points Z , we can essentially quickly find \hat{X} based on $K^{(X,Z)}$.
 91 (See [section 4](#) for more details.) That is, the set of proxy points Z can serve as a set of
 92 auxiliary points based on which the representative points can be quickly identified. In
 93 another word, when considering the interaction $K^{(X,Y)}$ between X and Y , we can use
 94 the interaction $K^{(X,Z)}$ between X and the proxy points Z to extract the contribution
 95 \hat{X} from X .

96 Thus, the proxy point method is a very convenient and useful tool for researchers
 97 working on kernel matrices. However, this elegant method is much less known in the
 98 numerical linear algebra community. Indeed, even the compression of some special
 99 Cauchy matrices (corresponding to a simple kernel) takes quite some efforts in matrix
 100 computations [\[34, 39, 49\]](#). In a recent literature survey [\[24\]](#) that lists many low-rank
 101 approximation methods (including a method for kernel matrices), the proxy point
 102 method is not mentioned at all. One reason that the proxy point method is not
 103 widely known by researchers in matrix computation is the lack of intuitive algebraic
 104 understanding of the background.

105 Moreover, in contrast with the success of the proxy point method in various
 106 practical applications, its theoretical justifications are still lacking in the literature.
 107 Potential theory [\[25, Chapter 6\]](#) can be used to explain the choice of proxy surface
 108 Γ in [Step 1 of Algorithm 1.1](#) when dealing with some PDE kernels (when $\kappa(x, y)$ is
 109 the fundamental solution of a PDE). However, there is no clear justification of the
 110 accuracy of the resulting low-rank approximation. Specifically, a clear explanation
 111 of such a simple procedure in terms of both the approximation error and the proxy
 112 point selection desired, especially from the linear algebra point of view.

113 Thus, we intend to seek a convenient way to *understand the proxy point method*
 114 and its accuracy based on some kernels. The following types of errors will be consid-
 115 ered (the notation will be made more precise later):

- 116 • The error ε for the approximation of kernel functions $\kappa(x, y)$ with the aid of
 117 proxy points.
- 118 • The error \mathcal{E} for the low-rank approximation of kernel matrices $K^{(X,Y)}$ via the
 119 proxy point method.
- 120 • The error \mathcal{R} for practical hybrid low-rank approximations of $K^{(X,Y)}$ based
 121 on the proxy point method.

122 Our main objectives are as follows.

- 123 1. Provide an intuitive explanation of the proxy point method using contour
 124 integration so as to make this elegant method more accessible to the numerical
 125 linear algebra community.
- 126 2. Give systematic analysis of the approximation errors of the proxy point
 127 method as well as the hybrid compression. We show how the kernel function
 128 approximation error ε and the low-rank compression error \mathcal{E} decay exponen-

129 tially with respect to the number of proxy points. We also show how our
 130 bounds for the error \mathcal{E} are nearly independent of the geometries and sizes of
 131 X and Y and why a bound for the error \mathcal{R} may be independent of one set
 132 (say, Y).

133 3. Use the error analysis to choose a nearly optimal set of proxy points in the
 134 low-rank kernel matrix compression. Our error bounds give a clear guideline
 135 to control the errors and to choose the locations of the proxy points so as
 136 to find nearly minimum errors. We also give a practical method to quickly
 137 estimate the optimal locations.

138 We conduct such studies based on kernels of the form

$$139 \quad (1.3) \quad \kappa(x, y) = \frac{1}{(x - y)^d}, \quad x, y \in \mathbb{C}, \quad x \neq y,$$

140 where d is a positive integer. Such kernels and their variants are very useful in
 141 PDE and integral equation solutions, structured ODE solutions [4], Cauchy matrix
 142 computations [39], Toeplitz matrix direct solutions [6, 34, 49], structured divide-and-
 143 conquer Hermitian eigenvalue solutions [17, 45], etc. Our derivations and analysis
 144 may also be useful for studying other kernels and higher dimensions. This will be
 145 considered in future work. (Note that the issue of what kernels the proxy point
 146 method can apply to is not the focus here.)

147 We would like to point out that several of our results like the error analyses in
 148 sections 3 and 4 can be easily extended to more general kernels and/or with other ap-
 149 proximation methods, as long as a relative approximation error for the kernel function
 150 approximation is available. Thus, our studies are useful for more general situations.

151 Our theoretical studies are also accompanied by various intuitive numerical tests
 152 which show that the error bounds nicely capture the error behaviors and also predict
 153 the location of the minimum errors.

154 In the remaining discussions, section 2 is devoted to an intuitive derivation of the
 155 proxy point method via contour integration and the analysis of the accuracy (ε) for the
 156 approximation of the kernel functions. The analytical low-rank compression accuracy
 157 (\mathcal{E}) and the nearly optimal proxy point selection are given in section 3. The study is
 158 further extended to the analysis of the hybrid low-rank approximation accuracy (\mathcal{R})
 159 with representative point selection in section 4. In section 5, the connection between
 160 the proxy point method and the Nyström method is discussed. Some notation we use
 161 frequently in the paper is listed below.

- 162 • The sets under consideration are $X = \{x_j\}_{j=1}^m$ and $Y = \{y_j\}_{j=1}^n$. $Z = \{z_j\}_{j=1}^N$
 163 is the set of proxy points.
- 164 • $\mathcal{C}(a; \gamma)$, $\mathcal{D}(a; \gamma)$, and $\bar{\mathcal{D}}(a; \gamma)$ denote respectively the circle, open disk, and
 165 closed disk with center $a \in \mathbb{C}$ and radius $\gamma > 0$.
- 166 • $\mathcal{A}(a; \gamma_1, \gamma_2) = \{z : \gamma_1 < |z - a| < \gamma_2\}$ with $0 < \gamma_1 < \gamma_2$ is an open annulus
 167 region.
- 168 • $K^{(X, Y)}$ is the $m \times n$ kernel matrix $(\kappa(x_i, y_j)_{x_i \in X, y_j \in Y})$ with $\kappa(x, y)$ in (1.3).
 169 Notation such as $K^{(X, Z)}$ and $K^{(\hat{X}, Z)}$ will also be used and can be understood
 170 similarly.

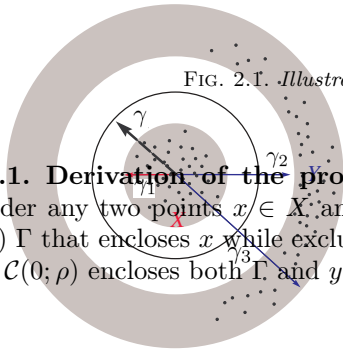
171 **2. The proxy point method for kernel function approximation and its**
 172 **accuracy.** In this section, we show one intuitive derivation of the proxy point method
 173 for the analytical approximation of the kernel functions, followed by detailed approx-
 174 imation error analysis.

175 Note that the kernel function (1.3) is translation invariant, i.e., $\kappa(x - z, y - z) =$

176 $\kappa(x, y)$ for any $x \neq y$ and $z \in \mathbb{C}$. Thus, the points X can be moved to be clustered
 177 around the origin. Without loss of generality, we always assume $X \subset \mathcal{D}(0; \gamma_1)$ and $Y \subset$
 178 $\mathcal{A}(0; \gamma_2, \gamma_3)$, where the radii satisfy $0 < \gamma_1 < \gamma_2 < \gamma_3$. See Figure 2.1. This condition
 179 is used to characterize the separation of the sets X and Y so as to theoretically
 180 guarantee the numerical low-rankness, as often used in applications of the FMM and
 181 rank structured matrix methods. In these methods, the points are hierarchically
 182 partitioned into subsets, and the interaction between one subset and those points
 183 that are a certain distance away is considered to be numerically low rank. See [15]
 184 for some illustrative figures. More discussions on this will be given in section 5.

FIG. 2.1. Illustration of γ , γ_1 , γ_2 , γ_3 , X , and Y .

185 **2.1. Derivation of the proxy point method via contour integration.**
 186 Consider any two points $x \in X$ and $y \in Y$. Draw a Jordan curve (a simple closed
 187 curve) Γ that encloses x while excluding y , and let $\rho > 0$ be large enough so that the
 circle $\mathcal{C}(0; \rho)$ encloses both Γ and y . See Figure 2.2a.

FIG. 2.2. Approximating the interaction $\kappa(x, y)$ by $\tilde{\kappa}(x, y)$ in (2.3) using proxy points.

188 Define the domain Ω_ρ to be the open region inside $\mathcal{C}(0; \rho)$ and outside Γ . Its
 189 boundary is $\partial\Omega_\rho := \mathcal{C}(0; \rho) \cup (-\Gamma)$, where $-\Gamma$ denotes the curve Γ in its negative
 190 direction. Now consider the function $f(z) := \kappa(x, z)$ on the closed domain $\bar{\Omega}_\rho :=$
 191 $\Omega_\rho \cup \partial\Omega_\rho$. The only singularity of $f(z)$ is at (z_j, \bar{y}) where $x \notin \bar{\Omega}_\rho$. Thus, $f(z)$ is analytic (or
 192 $\mathcal{C}(0; \rho)$ $\mathcal{C}(0; \rho)$)

193 holomorphic) on $\bar{\Omega}_\rho$. By the Cauchy integral formula [41],

$$194 \quad (2.1) \quad \kappa(x, y) = f(y) = \frac{1}{2\pi\mathbf{i}} \int_{\partial\Omega_\rho} \frac{f(z)}{z - y} dz = \frac{1}{2\pi\mathbf{i}} \int_{\mathcal{C}(0;\rho)} \frac{\kappa(x, z)}{z - y} dz - \frac{1}{2\pi\mathbf{i}} \int_{\Gamma} \frac{\kappa(x, z)}{z - y} dz,$$

195 where $\mathbf{i} = \sqrt{-1}$. Note that

$$196 \quad \left| \int_{\mathcal{C}(0;\rho)} \frac{\kappa(x, z)}{z - y} dz \right| \leq 2\pi\rho \cdot \max_{z \in \mathcal{C}(0;\rho)} \left| \frac{1}{(x - z)^d (z - y)} \right| \leq \frac{2\pi\rho}{(\rho - |x|)^d (\rho - |y|)},$$

198 where the right-hand side goes to zero when $\rho \rightarrow \infty$. Thus,

$$199 \quad \lim_{\rho \rightarrow \infty} \int_{\mathcal{C}(0;\rho)} \frac{\kappa(x, z)}{z - y} dz = 0.$$

200 Take the limit on (2.1) for $\rho \rightarrow \infty$, and the first term on the right-hand side vanishes.

201 We get

$$202 \quad (2.2) \quad \kappa(x, y) = \frac{1}{2\pi\mathbf{i}} \int_{\Gamma} \frac{\kappa(x, z)}{y - z} dz.$$

203 Note that this result is different from the Cauchy integral formula in that the point y
204 under consideration is outside the contour Γ in the integral.

205 To numerically approximate the contour integral (2.2), pick an N -point quadrature rule with quadrature points $\{z_j\}_{j=1}^N \subset \Gamma$ and the corresponding quadrature
206 weights $\{\omega_j\}_{j=1}^N$. Denoted by $\tilde{\kappa}(x, y)$ the approximation induced by such a quadrature
207 integration:

$$208 \quad (2.3) \quad \tilde{\kappa}(x, y) = \frac{1}{2\pi\mathbf{i}} \sum_{j=1}^N \omega_j \frac{\kappa(x, z_j)}{y - z_j} \equiv \sum_{j=1}^N \kappa(x, z_j) \phi_j(z_j, y), \quad \text{with} \quad \phi_j(z, y) = \frac{\omega_j}{2\pi\mathbf{i}(y - z)}.$$

210 Clearly, $\tilde{\kappa}(x, y)$ in (2.3) is a degenerate approximation to $\kappa(x, y)$ like (1.1). More-
211 over, it has one additional property of *structure preservation*: the function $\varphi_j(x)$ in
212 this case is $\kappa(x, z_j)$, which is exactly the original kernel $\kappa(x, y)$ with z_j in the role of
213 y . This gives a simple and intuitive explanation of the use of proxy points: the inter-
214 action between x and y can essentially be approximated by the interaction between x
215 and some proxy points Z (and later we will further see that Z can be independent of
216 the number of x and y points). These two interactions are made equivalent (in terms
217 of computing potential) through the use of the function ϕ_j . In another word, equiv-
218 alent charges can be placed on the proxy surface. A pictorial illustration is shown in
219 Figure 2.2b.

220 **2.2. Approximation error analysis.** Although the approximation (2.3) holds
221 for any proxy surface Γ satisfying the given conditions and for any quadrature rule,
222 we still need to make specific choices in order to obtain a more practical error bound.
223 Firstly, we assume the proxy surface to be a circle: $\Gamma = \mathcal{C}(0; \gamma)$, which is one of the
224 most popular choices in related work and is also consistent with our assumptions at
225 the beginning of section 2. For now, the proxy surface Γ is only assumed to be between
226 X and Y , i.e., $\gamma_1 < \gamma < \gamma_2$ as in Figure 2.1, and we will come back to discuss more
227 on this later. Secondly, the quadrature rule is chosen to be the composite trapezoidal
228 rule with

$$229 \quad (2.4) \quad z_j = \gamma \exp \left(\frac{2j\pi\mathbf{i}}{N} \right), \quad \omega_j = \frac{2\pi\mathbf{i}}{N} z_j, \quad j = 1, 2, \dots, N.$$

230 This choice can be justified by noting that the trapezoidal rule converges exponentially fast if applied to a periodic integrand [43]. Our results later also align with
 231 this. Moreover, if no specific direction is more important than others, the trapezoidal
 232 rule performs uniformly well on all directions of the complex plane \mathbb{C} . Some related
 233 discussions of this issue can be found in [23, 51].

234 As a result of the above assumptions, the function $\phi_j(z, y)$ in (2.3) becomes the
 235 following form:

$$237 \quad \phi(z, y) = \frac{1}{N} \frac{z}{y - z}, \quad y \neq z,$$

238 where we dropped the subscript j since j does not explicitly appear on the right-hand
 239 side. Also, we define

$$240 \quad g(z) = \frac{1}{z - 1}, \quad z \neq 1.$$

241 The following lemma will be used in the analysis of the approximation error for
 242 $\kappa(x, y)$.

243 **LEMMA 2.1.** *Let $\{z_j\}_{j=1}^N$ be the points defined in (2.4). Then the following result
 244 holds for all $z \in \mathbb{C} \setminus \{z_j\}_{j=1}^N$:*

$$245 \quad (2.5) \quad \sum_{j=1}^N \frac{z_j}{z - z_j} = N g\left(\left(\frac{z}{\gamma}\right)^N\right).$$

246 *Proof.* For any integer p , we have

$$247 \quad (2.6) \quad \sum_{j=1}^N z_j^p = \begin{cases} N\gamma^p, & \text{if } p \text{ is a multiple of } N, \\ 0, & \text{otherwise.} \end{cases}$$

248 If $|z| < \gamma$, then $|z/z_j| < 1$ for $j = 1, 2, \dots, N$ and

$$\begin{aligned} 249 \quad \sum_{j=1}^N \frac{z_j}{z - z_j} &= - \sum_{j=1}^N \frac{1}{1 - z/z_j} = - \sum_{j=1}^N \sum_{k=0}^{\infty} \left(\frac{z}{z_j}\right)^k = - \sum_{k=0}^{\infty} \left(z^k \sum_{j=1}^N z_j^{-k}\right) \\ 250 \quad &= - \sum_{l=0}^{\infty} z^{lN} N \gamma^{-lN} \quad (\text{with (2.6), only } k = lN \text{ terms left}) \\ 251 \quad &= - \frac{N}{1 - z^N/\gamma^N} = N g\left(\left(\frac{z}{\gamma}\right)^N\right). \end{aligned}$$

253 If $|z| > \gamma$, then $|z_j/z| < 1$ for $j = 1, 2, \dots, N$ and

$$\begin{aligned} 254 \quad \sum_{j=1}^N \frac{z_j}{z - z_j} &= \sum_{j=1}^N \left(\frac{z}{z - z_j} - 1 \right) = -N + \sum_{j=1}^N \frac{z}{z - z_j} = -N + \sum_{j=1}^N \frac{1}{1 - z_j/z} \\ 255 \quad &= -N + \sum_{j=1}^N \sum_{k=0}^{\infty} \left(\frac{z_j}{z}\right)^k = -N + \sum_{k=0}^{\infty} \left(z^{-k} \sum_{j=1}^N z_j^k\right) \\ 256 \quad &= -N + \sum_{l=0}^{\infty} z^{-lN} N \gamma^{lN} \quad (\text{with (2.6), only } k = lN \text{ terms left}) \\ 257 \quad &= -N + \frac{N}{1 - \gamma^N/z^N} = \frac{N}{z^N/\gamma^N - 1} = N g\left(\left(\frac{z}{\gamma}\right)^N\right). \end{aligned}$$

259 Finally, since both sides of (2.5) are analytic functions on $\mathbb{C} \setminus \{z_j\}_{j=1}^N$ and they
 260 agree on z with $|z| \neq \gamma$, by continuity, they must also agree on z when $|z| = \gamma$, $z \notin$
 261 $\{z_j\}_{j=1}^N$. This completes the proof. \square

262 In the following theorem, we derive an analytical expression for the accuracy of
 263 approximating $\kappa(x, y)$ by $\tilde{\kappa}(x, y)$. Without loss of generality, assume $x \neq 0$.

264 THEOREM 2.2. *Suppose $\kappa(x, y)$ in (1.3) is approximated by $\tilde{\kappa}(x, y)$ in (2.3) which
 265 is obtained from the composite trapezoidal rule with (2.4). Assume $x \neq 0$. Then*

266 (2.7)
$$\tilde{\kappa}(x, y) = \kappa(x, y) (1 + \varepsilon(x, y)),$$

267 where $\varepsilon(x, y)$ is the relative approximation error

268 (2.8)
$$\varepsilon(x, y) := \frac{\tilde{\kappa}(x, y) - \kappa(x, y)}{\kappa(x, y)} = g\left(\left(\frac{y}{\gamma}\right)^N\right) + \sum_{j=0}^{d-1} \frac{(y-x)^j}{j!} \frac{d^j}{dx^j} g\left(\left(\frac{\gamma}{x}\right)^N\right).$$

269 *Proof.* We prove this theorem by induction on d . For $d = 1$, substituting (2.4)
 270 into (2.3) yields

271
$$\begin{aligned} \tilde{\kappa}(x, y) &= \frac{1}{N} \sum_{j=1}^N \frac{z_j}{(x-z_j)(y-z_j)} = \frac{1}{N(x-y)} \sum_{j=1}^N \frac{(x-z_j) - (y-z_j)}{(x-z_j)(y-z_j)} z_j \\ 272 &= \frac{1}{N(x-y)} \left(\sum_{j=1}^N \frac{z_j}{y-z_j} - \sum_{j=1}^N \frac{z_j}{x-z_j} \right) \\ 273 &= \frac{1}{N(x-y)} \left(Ng\left(\left(\frac{y}{\gamma}\right)^N\right) - Ng\left(\left(\frac{x}{\gamma}\right)^N\right) \right) \quad (\text{Lemma 2.1}) \\ 274 &= \frac{1}{x-y} \left[1 + g\left(\left(\frac{y}{\gamma}\right)^N\right) + g\left(\left(\frac{\gamma}{x}\right)^N\right) \right]. \end{aligned}$$

276 Thus, (2.7) holds for $d = 1$.

277 Now suppose (2.7) holds for $d = k$ with k a positive integer. Equating (2.3) and
 278 (2.7) (with $d = k$) and plugging in $\kappa(x, y)$ to get

279
$$\sum_{j=1}^N \frac{\phi_j(z_j, y)}{(x-z_j)^k} = \frac{1}{(x-y)^k} \left[1 + g\left(\left(\frac{y}{\gamma}\right)^N\right) + \sum_{j=0}^{k-1} \frac{(y-x)^j}{j!} \frac{d^j}{dx^j} g\left(\left(\frac{\gamma}{x}\right)^N\right) \right].$$

280 The derivatives of the left and right-hand sides with respect to x are, respectively,
 281 $-k \sum_{j=1}^N \frac{\phi_j(z_j, y)}{(x-z_j)^{k+1}}$ and

282
$$\begin{aligned} &\frac{-k}{(x-y)^{k+1}} \left[1 + g\left(\left(\frac{y}{\gamma}\right)^N\right) + \sum_{j=0}^{k-1} \frac{(y-x)^j}{j!} \frac{d^j}{dx^j} g\left(\left(\frac{\gamma}{x}\right)^N\right) \right] \\ 283 &+ \frac{1}{(x-y)^k} \left[\sum_{j=0}^{k-1} \frac{(y-x)^j}{j!} \frac{d^{j+1}}{dx^{j+1}} g\left(\left(\frac{\gamma}{x}\right)^N\right) - \sum_{j=1}^{k-1} \frac{(y-x)^{j-1}}{(j-1)!} \frac{d^j}{dx^j} g\left(\left(\frac{\gamma}{x}\right)^N\right) \right] \\ 284 &= \frac{-k}{(x-y)^{k+1}} \left[1 + g\left(\left(\frac{y}{\gamma}\right)^N\right) + \sum_{j=0}^{k-1} \frac{(y-x)^j}{j!} \frac{d^j}{dx^j} g\left(\left(\frac{\gamma}{x}\right)^N\right) \right] \end{aligned}$$

$$\begin{aligned}
285 \quad & + \frac{1}{(x-y)^k} \frac{(y-x)^{k-1}}{(k-1)!} \frac{d^k}{dx^k} g\left(\left(\frac{\gamma}{x}\right)^N\right) \quad (\text{all terms cancel except for } j = k-1) \\
286 \quad & = \frac{-k}{(x-y)^{k+1}} \left[1 + g\left(\left(\frac{y}{\gamma}\right)^N\right) + \sum_{j=0}^k \frac{(y-x)^j}{j!} \frac{d^j}{dx^j} g\left(\left(\frac{\gamma}{x}\right)^N\right) \right]. \\
287
\end{aligned}$$

288 Thus,

$$289 \quad \sum_{j=1}^N \frac{\phi(z_j, y)}{(x-z_j)^{k+1}} = \frac{1}{(x-y)^{k+1}} \left[1 + g\left(\left(\frac{y}{\gamma}\right)^N\right) + \sum_{j=0}^k \frac{(y-x)^j}{j!} \frac{d^j}{dx^j} g\left(\left(\frac{\gamma}{x}\right)^N\right) \right].$$

290 That is, (2.7) holds for $d = k+1$. By induction, (2.7)–(2.8) are true for any positive
291 integer d . \square

292 With the analytical expression (2.8) we can give a rigorous upper bound for the
293 approximation error.

294 THEOREM 2.3. Suppose $0 < |x| < \gamma_1 < \gamma < |y|$. With all the assumptions
295 in Theorem 2.2, there exists a positive integer N_1 such that for any $N > N_1$, the
296 approximation error (2.8) is bounded by

$$297 \quad (2.9) \quad |\varepsilon(x, y)| \leq g\left(\left|\frac{y}{\gamma}\right|^N\right) + c g\left(\left|\frac{\gamma}{x}\right|^N\right),$$

298 where $c = 1$ if $d = 1$, and otherwise,

$$299 \quad (2.10) \quad c = 2 + 2 \sum_{j=1}^{d-1} \frac{[(|y/x| + 1)N]^j (2d)^{j-1}}{j!}.$$

300 *Proof.* For any positive integer N ,

$$301 \quad \left| g\left(\left(\frac{y}{\gamma}\right)^N\right) \right| = \frac{1}{|(|y/\gamma|^N) - 1|} \leq \frac{1}{|y/\gamma|^N - 1} = g\left(\left|\frac{y}{\gamma}\right|^N\right).$$

302 Thus, we only need to prove the following bound:

$$303 \quad (2.11) \quad \left| \sum_{j=0}^{d-1} \frac{(y-x)^j}{j!} \frac{d^j}{dx^j} g\left(\left(\frac{\gamma}{x}\right)^N\right) \right| \leq c g\left(\left|\frac{\gamma}{x}\right|^N\right).$$

304 When $d = 1$, it's easy to verify that the above inequality holds for $c = 1$ and any
305 positive integer N . We now consider the case when $d \geq 2$.

306 It can be verified that, for any positive integer i ,

$$307 \quad (2.12) \quad \frac{d}{dx} g^i \left(\left(\frac{\gamma}{x}\right)^N \right) = \frac{iN}{x} \left[g^i \left(\left(\frac{\gamma}{x}\right)^N \right) + g^{i+1} \left(\left(\frac{\gamma}{x}\right)^N \right) \right],$$

308 where g^i denotes function g raised to power i . Hence, the derivatives appearing in
309 (2.11) all have the following form:

$$310 \quad (2.13) \quad \frac{d^j}{dx^j} g \left(\left(\frac{\gamma}{x}\right)^N \right) = \frac{1}{x^j} \sum_{i=1}^{j+1} \alpha_i^{(j)} g^i \left(\left(\frac{\gamma}{x}\right)^N \right),$$

311 where $\alpha_i^{(j)}$ ($1 \leq i \leq j+1, 0 \leq j \leq d-1$) are constants.

312 We claim that, when $N > d$ and for any $0 \leq j \leq d - 1$, there exist constants $\beta^{(j)}$
 313 dependent on d so that

$$314 \quad |\alpha_i^{(j)}| \leq \beta^{(j)} N^j, \quad 1 \leq i \leq j+1.$$

315 This claim can be proved by induction on j . It is obviously true when $j = 0$, and
 316 $\beta^{(0)} = 1$ in this case. When $j = 1$, (2.12) means that the claim is true with $\alpha_1^{(1)} =$
 317 $\alpha_2^{(1)} = N$ and $\beta^{(1)} = 1$. Suppose the claim holds for $j = k$ with $1 \leq k \leq d - 2$ (where
 318 we also assume $d > 2$, since otherwise the claim is already proved). Then

325 Thus, the coefficients satisfy the following recurrence relation

$$\alpha_i^{(k+1)} = \begin{cases} (N-k)\alpha_1^{(k)}, & i = 1, \\ (iN-k)\alpha_i^{(k)} + N(i-1)\alpha_{i-1}^{(k)}, & 2 \leq i \leq k+1, \\ N(k+1)\alpha_{k+1}^{(k)}, & i = k+2. \end{cases}$$

327 Therefore, when $N > d$, we can pick (conservatively)

$$328 \quad (2.14) \quad \beta^{(k+1)} = 2d\beta^{(k)},$$

329 so that $|\alpha_i^{(k+1)}| \leq \beta^{(k+1)} N^{k+1}$. That is, the claim holds for $j = k+1$ and this finishes
 330 the induction.

331 Now, we go back to prove (2.11). By (2.13),

$$\begin{aligned}
& \text{332} \quad \left| \sum_{j=0}^{d-1} \frac{(y-x)^j}{j!} \frac{d^j}{dx^j} g\left(\left(\frac{\gamma}{x}\right)^N\right) \right| = \left| \sum_{j=0}^{d-1} \left[\frac{(y-x)^j}{j!} \frac{1}{x^j} \sum_{i=1}^{j+1} \alpha_i^{(j)} g^i \left(\left(\frac{\gamma}{x}\right)^N\right) \right] \right| \\
& \text{333} \quad \leq \sum_{j=0}^{d-1} \left[\frac{(|y/x|+1)^j}{j!} \sum_{i=1}^{j+1} |\alpha_i^{(j)}| g^i \left(\left|\frac{\gamma}{x}\right|^N\right) \right] \leq \sum_{j=0}^{d-1} \left[\frac{(|y/x|+1)^j}{j!} \beta^{(j)} N^j \sum_{i=1}^{j+1} g^i \left(\left|\frac{\gamma}{x}\right|^N\right) \right]. \\
& \text{334}
\end{aligned}$$

335 Set

$$336 \quad (2.16) \quad N_1 = \max\{d, \lceil \log 3 / \log |\gamma_1/x| \rceil\}.$$

337 Then for $N > N_1$, $|\gamma/x|^N > |\gamma_1/x|^N > 3$ and $g(|\gamma/x|^N) < 1/2$. Thus, for $1 \leq j \leq$
 338 $d-1$,

$$339 \quad \sum_{i=1}^{j+1} g^i \left(\left| \frac{\gamma}{x} \right|^N \right) \leq 2g \left(\left| \frac{\gamma}{x} \right|^N \right).$$

340 Continuing on (2.15), for $N > N_1$, we get

$$341 \quad (2.17) \quad \left| \sum_{j=0}^{d-1} \frac{(y-x)^j}{j!} \frac{d^j}{dx^j} g \left(\left(\frac{\gamma}{x} \right)^N \right) \right| \leq cg \left(\left| \frac{\gamma}{x} \right|^N \right), \quad \text{with } c = 2 \sum_{j=0}^{d-1} \frac{(|y/x|+1)^j}{j!} \beta^{(j)} N^j.$$

342 Note that with the way $\beta^{(j)}$ is picked as in (2.14), $\beta^{(j)}$ satisfies

$$343 \quad \beta^{(j)} = (2d)^{j-1} \beta^{(1)} = (2d)^{j-1}, \quad j = 1, 2, \dots, d-1.$$

344 Then c in (2.17) becomes (2.10). Thus, (2.11) holds with c in (2.10). \square

345 The upper bound (2.9) in Theorem 2.3 has two implications.

- Since $g(|y/\gamma|^N)$ and $g(|\gamma/x|^N)$ decay almost exponentially with N and c is just a polynomial in N , d , and $|y/x|$ with degrees up to $d-1$, the bound in (2.9) decays roughly exponentially as N increases.
- The bound can help us identify a nearly optimal radius γ of the proxy surface Γ so as to minimize the error. This is given in the following theorem.

351 THEOREM 2.4. Suppose $0 < |x| < \gamma_1 < |y|$ and $\kappa(x, y)$ in (1.3) is approximated
 352 by $\tilde{\kappa}(x, y)$ in (2.3) with (2.4). If the upper bound in (2.9) is viewed as a real function
 353 in γ on the interval $(|x|, |y|)$, then there exists a positive integer N_2 independent of γ ,
 354 such that for $N > N_2$,

1. this upper bound has a unique minimizer $\gamma^* \in (|x|, |y|)$;
2. the minimum of this upper bound decays asymptotically as $\mathcal{O}(|y/x|^{-N/2})$.

357 *Proof.* To find the minimizer, we just need to consider the real function

$$358 \quad h(t) = \frac{1}{b/t-1} + \frac{c}{t/a-1}, \quad t \in (a, b),$$

359 where $a = |x|^N$, $b = |y|^N$, and c is either equal to 1 (for $d = 1$) or defined in (2.10)
 360 (for $d \geq 2$). The derivative of the function is

$$361 \quad h'(t) = \frac{p(t)}{(t-a)^2(t-b)^2}, \quad \text{with } p(t) = (b-ac)t^2 + 2ab(c-1)t + ab(a-bc).$$

362 Consider $p(t)$, which is a quadratic polynomial in t with the following properties.

- The coefficient of the second order term is

$$364 \quad b - ac = |x|^N (|y/x|^N - c).$$

365 Since c is either equal to 1 (for $d = 1$) or a polynomial in N , d , and $|y/x|$ with
 366 degrees up to $d-1$ (for $d \geq 2$), there exists N_2 larger than N_1 in Theorem 2.3
 367 such that $|y/x|^N > c$ for any $N > N_2$. Thus, $b - ac > 0$ for $N > N_2$.

- The discriminant is $4abc(a-b)^2 > 0$.
- When evaluated at $t = a$ and $t = b$, the function $p(t)$ gives respectively

$$370 \quad p(a) = -ac(a-b)^2 < 0, \quad p(b) = b(a-b)^2 > 0.$$

371 All the properties above combined indicate that $p(t)$ has one root $t_0 \in (a, b)$ and
 372 $h'(t) < 0$ on (a, t_0) and $h'(t) > 0$ on (t_0, b) . Thus, t_0 is the only zero of $p(t)$ in $[a, b]$
 373 and $\gamma^* = \sqrt[N]{t_0}$ is the unique minimizer of the upper bound in (2.9). The requirements
 374 for picking N_2 are $N_2 > N_1$ and $|y/x|^{N_2} > c$. Hence, N_2 is independent of γ .

375 To prove the second part of the theorem, we explicitly compute the root t_0 of
 376 $p(t) = 0$ in (a, b) and substitute it into $h(t)$ to get

$$377 \quad h(t_0) = \frac{2\sqrt{cb/a} + (c+1)}{b/a - 1} = \frac{2\sqrt{c}|y/x|^{N/2} + (c+1)}{|y/x|^N - 1} \sim \mathcal{O}\left(\left|\frac{y}{x}\right|^{-N/2}\right),$$

378 The details involve tedious algebra and are omitted here. \square

379 In the proof, we can actually find the minimizer but are not explicitly writing it
 380 out. The reason is that the minimizer depends on x and y and it makes more sense
 381 to write a minimizer later when we consider the low-rank approximation of the kernel
 382 matrix. See the next section.

383 **3. Low-rank approximation accuracy and proxy point selection in the**
 384 **proxy point method for kernel matrices.** With the kernel $\kappa(x, y)$ in (1.3) ap-
 385 proximated by $\tilde{\kappa}(x, y)$ in (2.3), a low-rank approximation to $K^{(X, Y)}$ in (1.2) as follows
 386 is obtained:

$$387 \quad (3.1) \quad K^{(X, Y)} \approx \tilde{K}^{(X, Y)} := (\tilde{\kappa}(x, y)_{x \in X, y \in Y}) = K^{(X, Z)} \Phi^{(Z, Y)},$$

388 where $\Phi^{(Z, Y)} = (\phi(z, y)_{z \in Z, y \in Y})$. The analysis in subsection 2.2 provides entrywise
 389 approximation errors for (3.1) (with implicit dependence on x). Now, we consider
 390 normwise approximation errors for $K^{(X, Y)}$ and obtain relative error bounds indepen-
 391 dent of the specific x and y points. The error analysis will be further used to estimate
 392 the optimal choice of the radius γ for the proxy surface in the low-rank approximation.
 393 We look at the cases $d = 1$ and $d \geq 2$ separately.

394 **3.1. The case $d = 1$.** In this case, the proof of Theorem 2.2 for $d = 1$ gives an
 395 explicit expression for the entrywise approximation error

$$396 \quad (3.2) \quad \varepsilon(x, y) = g\left(\left(\frac{\gamma}{x}\right)^N\right) + g\left(\left(\frac{y}{\gamma}\right)^N\right).$$

397 We then have the following result on the low-rank approximation error in Frobenius
 398 norm.

399 **PROPOSITION 3.1.** *Suppose $d = 1$ and $\kappa(x, y)$ in (1.3) is approximated by $\tilde{\kappa}(x, y)$
 400 in (2.3) with (2.4). If $0 < |x| < \gamma_1 < \gamma < \gamma_2 < |y|$ for all $x \in X, y \in Y$, then for any
 401 $N > 0$,*

$$402 \quad (3.3) \quad \frac{\|\tilde{K}^{(X, Y)} - K^{(X, Y)}\|_F}{\|K^{(X, Y)}\|_F} \leq g\left(\left(\frac{\gamma}{\gamma_1}\right)^N\right) + g\left(\left(\frac{\gamma_2}{\gamma}\right)^N\right).$$

403 *Moreover, if the upper bound on the right-hand side is viewed as a function in γ , it has
 404 a unique minimizer $\gamma^* = \sqrt{\gamma_1 \gamma_2}$ and the minimum is $2g\left((\gamma_2/\gamma_1)^{N/2}\right)$ which decays
 405 asymptotically as $\mathcal{O}(|\gamma_2/\gamma_1|^{-N/2})$.*

406 *Proof.* The approximation error bound (3.3) is a direct application of the entry-
 407 wise error in (3.2) together with the fact that $g(t)$ monotonically decreases for $t > 1$.

408 To find the minimizer of the right-hand side of (3.3), we can either follow the
 409 proof in [Theorem 2.4](#) or simply use the following explicit expression:

$$410 \quad g((\gamma/\gamma_1)^N) + g((\gamma_2/\gamma)^N) = \frac{1}{(\gamma/\gamma_1)^N - 1} + \frac{1}{(\gamma_2/\gamma)^N - 1} \\ 411 \quad = -1 + \frac{(\gamma_2/\gamma_1)^N - 1}{(\gamma_2/\gamma_1)^N + 1 - ((\gamma/\gamma_1)^N + (\gamma_2/\gamma)^N)}. \\ 412$$

413 We just need to minimize $(\gamma/\gamma_1)^N + (\gamma_2/\gamma)^N$, which reaches its minimum at $\gamma^* = \sqrt{\gamma_1\gamma_2}$. \square
 414

415 *Remark 3.2.* Although it is not easy to choose γ to minimize the approximation
 416 error directly, the minimizer γ^* for the bound in (3.3) can serve as a reasonable
 417 estimate of the minimizer for the error. These can be seen from an intuitive numerical
 418 example below. In addition, the minimum $2g((\gamma_2/\gamma_1)^{N/2})$ of the bound in (3.3)
 419 decays nearly exponentially as N increases. Thus, to reach a relative approximation
 420 accuracy τ , we can conveniently decide the number of proxy points:

$$421 \quad N = \mathcal{O}\left(\frac{\log(1/\tau)}{\log(\gamma_2/\gamma_1)}\right).$$

422 Clearly, N does not depend on the number of points or the geometries of X, Y . It
 423 only depends on τ and γ_2/γ_1 which indicates the separation of X and Y . This is
 424 consistent with the conclusions in the FMM context [42].

425 **EXAMPLE 1.** We use an example to illustrate the results in [Proposition 3.1](#) for
 426 $d = 1$. The points in X and Y are uniformly chosen from their corresponding regions
 427 and are plotted in [Figure 3.1a](#), where $m = |X| = 200$, $n = |Y| = 300$, $\gamma_1 = 0.5$,
 428 $\gamma_2 = 2$, and $\gamma_3 = 5$.

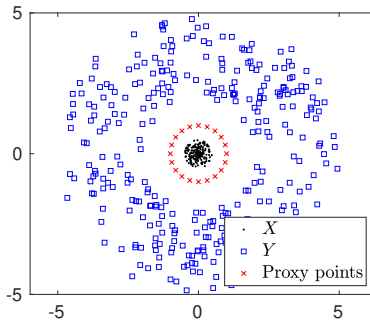
429 First, we fix the number of proxy points $N = 20$ and let γ vary. We plot the
 430 actual error $\mathcal{E}_N(\gamma) := \|\tilde{K}^{(X,Y)} - K^{(X,Y)}\|_F / \|K^{(X,Y)}\|_F$ and the error bound in (3.3).
 431 See [Figure 3.1b](#). We can see that both plots are V-shape lines and the error bound
 432 is a close estimate of the actual error. Moreover, the bound nicely captures the error
 433 behavior, and the actual error reaches its minimum almost at the same location where
 434 the error bound is minimized: $\gamma^* = \sqrt{\gamma_1\gamma_2} = 1$. Thus, γ^* is a nice choice to minimize
 435 the error. The proxy points Z with radius γ^* are plotted in [Figure 3.1a](#).

436 Then in [Figure 3.1c](#), we fix $\gamma = \gamma^*$ and let N vary. Again, the error bound
 437 provides a nice estimate for the error. Furthermore, both the error and the bound
 438 decay exponentially like $\mathcal{O}(|\gamma_2/\gamma_1|^{-N/2}) = \mathcal{O}(2^{-N})$.

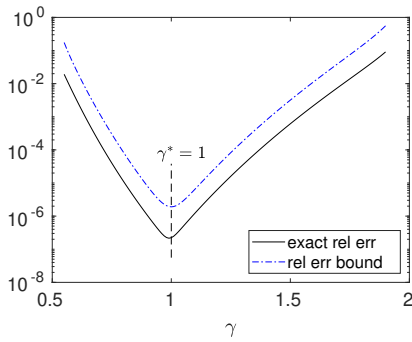
439 **3.2. The case $d > 2$.** In this case, there is no simple explicit formula for $\varepsilon(x, y)$
 440 like in (3.2). The results in [Theorems 2.3](#) and [2.4](#) cannot be trivially extended to
 441 study the normwise error either since no lower bound is imposed on $|x|$ in $|y/x|$.
 442 Nevertheless, we can derive a bound as follows.

443 **PROPOSITION 3.3.** *Suppose $d \geq 2$ and $\kappa(x, y)$ in (1.3) is approximated by $\tilde{\kappa}(x, y)$
 444 in (2.3) with (2.4). If $0 < |x| < \gamma_1 < \gamma < \gamma_2 < |y| < \gamma_3$ for all $x \in X, y \in Y$, then
 445 there exists a positive integer N_3 independent of γ such that for $N > N_3$,*

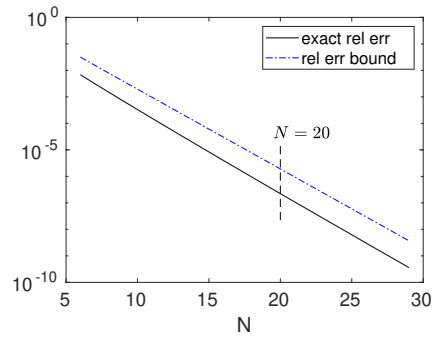
$$446 \quad (3.4) \quad \frac{\|\tilde{K}^{(X,Y)} - K^{(X,Y)}\|_F}{\|K^{(X,Y)}\|_F} \leq g\left(\left(\frac{\gamma_2}{\gamma}\right)^N\right) + \hat{c}g\left(\left(\frac{\gamma}{\gamma_1}\right)^N\right).$$



(a) Sets X and Y with $\gamma_1 = 0.5$, $\gamma_2 = 2$, $\gamma_3 = 5$ and proxy points Z selected with radius $\gamma^* = 1$



(b) Varying proxy surface radius γ



(c) Varying number of proxy points N

FIG. 3.1. *Example 1: For $d = 1$, the selection of the proxy points and the actual relative error $\mathcal{E}_N(\gamma)$ compared with its upper bound in Proposition 3.1 for different γ and N .*

447 where

$$448 \quad (3.5) \quad \hat{c} = 2 + 2 \sum_{j=1}^{d-1} \frac{[(|\gamma_3/\gamma_1| + 1)N]^j (2d)^{j-1}}{j!}.$$

449 Moreover, if the upper bound in (3.4) is viewed as a real function in γ on the interval
450 (γ_1, γ_2) , then

451 1. this upper bound has a unique minimizer

$$452 \quad (3.6) \quad \gamma^* = \left(\frac{(\gamma_2^N - \gamma_1^N) \sqrt{(\gamma_1 \gamma_2)^N \hat{c}} - (\gamma_1 \gamma_2)^N (\hat{c} - 1)}{\gamma_2^N - \gamma_1^N \hat{c}} \right)^{1/N} \in (\gamma_1, \gamma_2);$$

453 2. the minimum of this upper bound decays asymptotically as $\mathcal{O}(|\gamma_2/\gamma_1|^{-N/2})$.

454 *Proof.* Following the proof of Theorem 2.4, we can set N_3 to be the maximum of
455 N_2 in Theorem 2.4 for all $x \in X$. Based on the entrywise error bound in (2.9), we
456 can just show the following inequalities for $N > N_3$ and any $x \in X, y \in Y$:

$$457 \quad g\left(\left|\frac{y}{\gamma}\right|^N\right) < g\left(\left(\frac{\gamma_2}{\gamma}\right)^N\right), \quad cg\left(\left|\frac{\gamma}{x}\right|^N\right) < \hat{c}g\left(\left(\frac{\gamma}{\gamma_1}\right)^N\right).$$

458 The first inequality is obvious. We then focus on the second one. Just for the purpose
 459 of this proof, we write c in (2.10) as $c(|x|, |y|)$ to indicate its dependency on $|x|$ and
 460 $|y|$. $c(|x|, |y|)$ can be viewed as a degree- $(d-1)$ polynomial in $1/|x|$ and $|y|$ with all
 461 positive coefficients.

462 Write

$$463 \quad c(|x|, |y|) g\left(\left|\frac{\gamma}{x}\right|^N\right) = [c(|x|, |y|)|x|^{d-1}] \left[g\left(\left|\frac{\gamma}{x}\right|^N\right) |x|^{1-d}\right].$$

464 The first term $c(|x|, |y|)|x|^{d-1}$ is a polynomial in $|x|$ with all positive coefficients and
 465 increases with $|x|$. The second term is

$$466 \quad g\left(\left|\frac{\gamma}{x}\right|^N\right) |x|^{1-d} = \frac{|x|^{N-d+1}}{\gamma^N - |x|^N}.$$

467 With $N > N_3$, it can be shown that this term is also strictly increasing in $|x|$ for
 468 $0 < |x| < \gamma_1 < \gamma$.

469 Thus for any $x \in X, y \in Y$,

$$470 \quad c(|x|, |y|) g\left(\left|\frac{\gamma}{x}\right|^N\right) < c(\gamma_1, |y|) g\left(\left|\frac{\gamma}{\gamma_1}\right|^N\right) < c(\gamma_1, \gamma_3) g\left(\left|\frac{\gamma}{\gamma_1}\right|^N\right) = \hat{c} g\left(\left|\frac{\gamma}{\gamma_1}\right|^N\right),$$

471 where the constant \hat{c} is defined in (3.5) which is c in (2.10) with $|y/x|$ replaced by
 472 γ_3/γ_1 .

473 The minimizer γ^* in (3.6) for the upper bound is the root of a quadratic polyno-
 474 mial in (γ_1, γ_2) and can be obtained following the proof of [Theorem 2.4](#). \square

475 Based on this corollary, we can draw conclusions similar to those in [Remark 3.2](#).
 476 In addition, although γ_3 is needed so that Y is on a bounded domain in order to
 477 derive the error bound (3.4), we believe such an limitation is not needed in practice.
 478 In fact, the analytical compression tends to be more accurate when the points y are
 479 farther away from the set X . Also, if γ_3 is too large, then we may slightly shift the x
 480 points to make sure $|x|$ is larger than a positive number γ_0 so as to similarly derive
 481 an error bound using γ_0 instead of γ_3 .

482 **3.3. A practical method to estimate the optimal radius γ .** In [Propositions 3.1](#) and [3.3](#), the upper bounds are used to estimate the optimal choice of γ for
 483 the radius of the proxy surface. In practice, it is possible that the upper bound may
 484 be conservative, especially when $d > 1$. Thus, we also propose the following method
 485 to quickly obtain a numerical estimate of the optimal choice.

486 In [Propositions 3.1](#) and [3.3](#), the optimal γ^* is independent of the number of points
 487 in X and Y and their distribution. This feature motivates the idea to pick subsets
 488 $X_0 \subset \mathcal{D}(0; \gamma_1)$ and $Y_0 \subset \mathcal{A}(0; \gamma_2, \gamma_3)$ and use them to estimate the actual error. That
 489 is, we would expect the following two quantities to have similar behaviors when γ
 490 varies in (γ_1, γ_2) :

$$492 \quad (3.7) \quad \mathcal{E}_N^0(\gamma) := \frac{\|K^{(X_0, Y_0)} - \tilde{K}^{(X_0, Y_0)}\|_F}{\|K^{(X_0, Y_0)}\|_F}, \quad \mathcal{E}_N(\gamma) := \frac{\|K^{(X, Y)} - \tilde{K}^{(X, Y)}\|_F}{\|K^{(X, Y)}\|_F}.$$

493 $\mathcal{E}_N^0(\gamma)$ can be used as an estimator of the actual approximation error $\mathcal{E}_N(\gamma)$. Note
 494 that $K^{(X_0, Y_0)}$ and $\tilde{K}^{(X_0, Y_0)}$ are computable through (1.3) and (2.3), respectively, so
 495 $\mathcal{E}_N^0(\gamma)$ can be computed explicitly, and the cost is extremely small if $|X_0| \ll |X|$ and
 496 $|Y_0| \ll |Y|$.

497 Note that in rank-structured matrix computations, often an admissible condition
 498 or separation parameter is prespecified for the compression of multiple off-diagonal
 499 blocks. In the case of kernel matrices, it means that the process of estimating the
 500 optimal γ needs to be run only once and can then be used in multiple compression
 501 steps.

502 EXAMPLE 2. We use an example to demonstrate the numerical selection of the
 503 optimal γ . Consider $d = 2, 3$ and the two sets X and Y in [Example 1](#) with the same
 504 values $\gamma_1, \gamma_2, \gamma_3$ (see [Figure 3.1a](#)). Fix $N = 30$.

505 For the sets X_0 and Y_0 we choose, we set $l = |X_0| = |Y_0|$ to be 1, 2, or 3. We
 506 make sure $x = \gamma_1$ and $y = \gamma_2$ as points of \mathbb{C} are always in X_0 and Y_0 , respectively.
 507 Thus, $\mathcal{E}_N^0(\gamma)$ is more likely to capture the behavior of $\mathcal{E}_N(\gamma)$. Any additional points
 508 in X_0 are uniformly distributed in the circle $\mathcal{C}(0; \gamma_1)$ and any additional points in Y_0
 are uniformly distributed in $\mathcal{C}(0; \gamma_2)$.

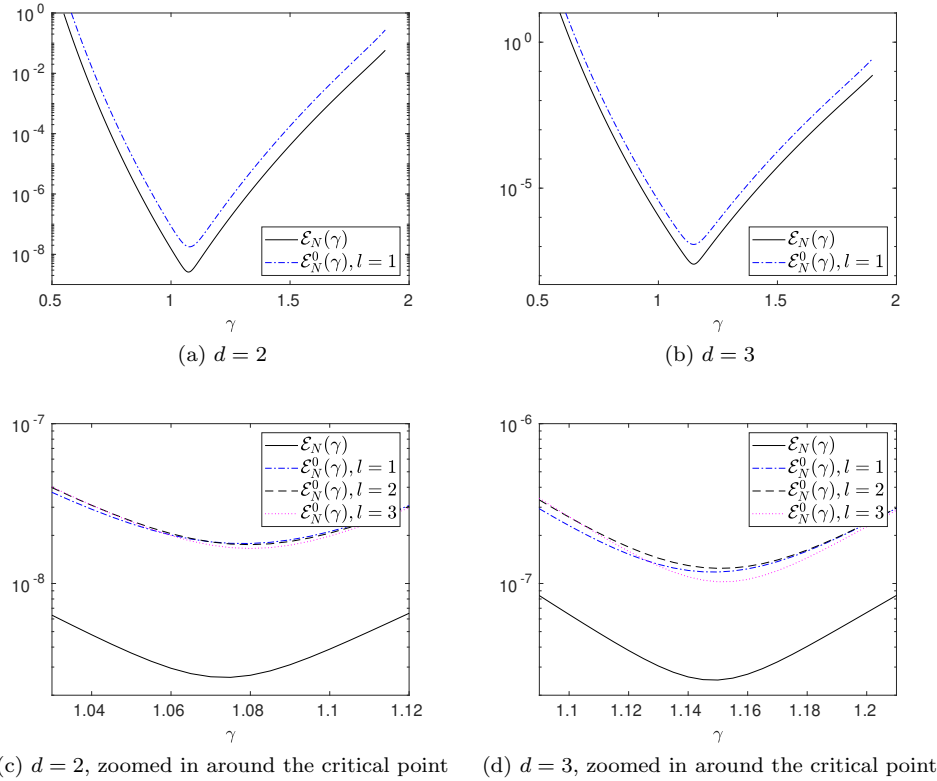


FIG. 3.2. *Example 2:* For $d = 2$ and 3, how the estimator $\mathcal{E}_N^0(\gamma)$ with $l = 1, 2, 3$ compare with the actual error $\mathcal{E}_N(\gamma)$.

509
 510 With $l = 1$, both $\mathcal{E}_N(\gamma)$ and $\mathcal{E}_N^0(\gamma)$ are plotted. See [Figures 3.2a](#) and [3.2b](#) for
 511 $d = 2$ and 3, respectively. We can see that $\mathcal{E}_N^0(\gamma)$ already gives a good estimate of
 512 the behavior of $\mathcal{E}_N(\gamma)$ for both cases. Then in [Figures 3.2c](#) and [3.2d](#) we plot $\mathcal{E}_N^0(\gamma)$
 513 for $l = 1, 2, 3$ and zoom in at around the minimum since they almost coincide with
 514 each other away from the minimum. The minimums of the three cases are very close
 515 to each other.

516 **4. Low-rank approximation accuracy in hybrid compression and rep-**
 517 **representative point selection.** The analytical compression in section 3 can serve as
 518 a preliminary low-rank approximation, which is typically followed by an algebraic
 519 compression step to get a more compact low-rank approximation. In this section,
 520 we analyze the approximation error of such hybrid (analytical/algebraic) compression
 521 method applied to $K^{(X,Y)}$.

522 Suppose $m = |X|$ and $n = |Y|$ are sufficiently large and $N = |Z|$ is fixed. With
 523 the preliminary low-rank approximation in (3.1), since $K^{(X,Z)}$ has a much smaller
 524 column size than $K^{(X,Y)}$, it becomes practical to apply an SRRQR factorization to
 525 $K^{(X,Z)}$ to obtain the following approximation:

526 (4.1)
$$K^{(X,Z)} \approx UK^{(\hat{X},Z)}, \quad \text{with } U = P \begin{pmatrix} I \\ E \end{pmatrix},$$

527 where P is a permutation matrix so that $K^{(\hat{X},Z)}$ a submatrix of $K^{(X,Z)}$ corresponding
 528 to a subset $\hat{X} \subset X$. \hat{X} can be referred to as a set of *representative points* of X . (4.1)
 529 is an interpolative decomposition of $K^{(X,Z)}$. It is also called structure-preserving
 530 rank-revealing (SPRR) factorization in [49] since $K^{(\hat{X},Z)}$ is a submatrix of $K^{(X,Z)}$.

531 Although U generally does not have orthonormal columns, the SRRQR factor-
 532 ization keeps its norm under control in the sense that entries of E have magnitudes
 533 bounded by a constant e (e.g., $e = 2$ or \sqrt{N}). See [18] for details.

534 We then have

535 (4.2a)
$$K^{(X,Y)} \approx \tilde{K}^{(X,Y)} = K^{(X,Z)}\Phi^{(Z,Y)} \quad (\text{by (2.3) and (3.1)})$$

536 (4.2b)
$$\approx UK^{(\hat{X},Z)}\Phi^{(Z,Y)} \quad (\text{by (4.1)})$$

537 (4.2c)
$$= U\tilde{K}^{(\hat{X},Y)} \quad (\text{by (2.3) and similar to (3.1)})$$

538 (4.2d)
$$\approx UK^{(\hat{X},Y)}, \quad (\text{by } \tilde{\kappa}(x,y) \approx \kappa(x,y))$$

540 which is an SPRR factorization of $K^{(X,Y)}$.

541 Similarly, an SRRQR factorization can further be applied to $K^{(\hat{X},Y)}$ to produce

542 (4.3)
$$K^{(\hat{X},Y)} \approx K^{(\hat{X},\hat{Y})}V^T, \quad \text{with } V = Q \begin{pmatrix} I \\ F \end{pmatrix},$$

543 where Q is a permutation matrix and $\hat{Y} \subset Y$. The approximation (4.2) together with
 544 (4.3) essentially enables us to quickly to select representative points from both X and
 545 Y . In another word, we have a skeleton factorization of $K^{(X,Y)}$ as

546 (4.4)
$$K^{(X,Y)} \approx UK^{(\hat{X},\hat{Y})}V^T.$$

547 Note that computing an SPRR or skeleton factorization for $K^{(X,Y)}$ directly (or to
 548 find a submatrix $K^{(\hat{X},\hat{Y})}$ with the largest “volume” [14, 44]) is typically prohibitively
 549 expensive for large m and n . Here, the proxy point method substantially reduces the
 550 cost. In fact, (4.2a) and (4.2c) are done analytically with no computation cost. Only
 551 the SRRQR factorizations of skinny matrices ($K^{(X,Z)}$ and/or $K^{(\hat{X},Y)}$) are needed.
 552 The total compression cost is $\mathcal{O}(mNr)$ for (4.2) or $\mathcal{O}(mNr + nr^2)$ for (4.4) instead
 553 of $\mathcal{O}(mnr)$ in the case of direct compression, where $r = |\hat{X}| \geq |\hat{Y}|$. As we have
 554 discussed before, N is only a constant independent of m and n . Thus, this procedure
 555 is significantly more efficient than applying SRRQR factorizations directly to the
 556 original kernel matrix.

557 The next theorem concerns the approximation error of the hybrid compression
 558 via either (4.2) or (4.4).

559 THEOREM 4.1. *Suppose $0 < |x| < \gamma_1 < \gamma < \gamma_2 < |y| < \gamma_3$ for any $x \in X, y \in Y$
 560 and the N proxy points in Z are located on the proxy surface with radius γ^* . Let $r =$
 561 $|\hat{X}|$ and let the relative tolerance in the kernel approximation be τ_1 (i.e., $|\varepsilon(x, y)| < \tau_1$
 562 for $\varepsilon(x, y)$ in (2.7)) and the relative approximation tolerance (in Frobenius norm) in
 563 the SRRQR factorizations (4.1) and (4.3) be τ_2 . Assume the entries of E in (4.1)
 564 and F in (4.3) have magnitudes bounded by e . Then the approximation of $K^{(X, Y)}$ by
 565 (4.2) satisfies*

566 (4.5)
$$\frac{\|K^{(X, Y)} - UK^{(\hat{X}, Y)}\|_F}{\|K^{(X, Y)}\|_F} < s_1\tau_1 + s_2\tau_2,$$

567 where

568
$$s_1 = 1 + \sqrt{r + (m - r)e^2} \sqrt{1 - \frac{(m - r)(\gamma_2 - \gamma_1)^{2d}}{m(\gamma_1 + \gamma_3)^{2d}}}, \quad s_2 = \frac{\gamma^*(\gamma_1 + \gamma_3)^d}{(\gamma_2 - \gamma^*)(\gamma^* - \gamma_1)^d}.$$

570 The approximation of $K^{(X, Y)}$ by (4.4) satisfies

571 (4.6)
$$\frac{\|K^{(X, Y)} - UK^{(\hat{X}, \hat{Y})}V^T\|_F}{\|K^{(X, Y)}\|_F} < s_1\tau_1 + \tilde{s}_2\tau_2,$$

572 where $\tilde{s}_2 = s_2 + s_1 - 1$.

573 *Proof.* The following inequalities for $x \in X, y \in Y, z \in Z$ will be useful in the
 574 proof:

575 (4.7)
$$|\phi(z, y)| < \frac{\gamma^*}{N(\gamma_2 - \gamma^*)},$$

576 (4.8)
$$|\kappa(x, z)| < \frac{1}{(\gamma^* - \gamma_1)^d},$$

577 (4.9)
$$\frac{1}{(\gamma_1 + \gamma_3)^d} < |\kappa(x, y)| < \frac{1}{(\gamma_2 - \gamma_1)^d}.$$

579 Note that

580 (4.10)
$$\begin{aligned} & \|K^{(X, Y)} - UK^{(\hat{X}, Y)}\|_F \\ & \leq \|K^{(X, Y)} - \tilde{K}^{(X, Y)}\|_F + \|\tilde{K}^{(X, Y)} - UK^{(\hat{X}, Y)}\|_F \\ & \leq \|K^{(X, Y)} - \tilde{K}^{(X, Y)}\|_F + \|\tilde{K}^{(X, Y)} - U\tilde{K}^{(\hat{X}, Y)}\|_F + \|U\tilde{K}^{(\hat{X}, Y)} - UK^{(\hat{X}, Y)}\|_F \\ & = \|K^{(X, Y)} - \tilde{K}^{(X, Y)}\|_F + \|K^{(X, Z)}\Phi^{(Z, Y)} - UK^{(\hat{X}, Z)}\Phi^{(Z, Y)}\|_F \\ & \quad + \|U\tilde{K}^{(\hat{X}, Y)} - UK^{(\hat{X}, Y)}\|_F \quad (\text{by (4.2a)–(4.2c)}) \\ & \leq \|K^{(X, Y)} - \tilde{K}^{(X, Y)}\|_F + \|K^{(X, Z)} - UK^{(\hat{X}, Z)}\|_F\|\Phi^{(Z, Y)}\|_F \\ & \quad + \|U\|_F\|K^{(\hat{X}, Y)} - \tilde{K}^{(\hat{X}, Y)}\|_F. \end{aligned}$$

588 Now, we derive upper bounds separately for the three terms in the last step above.

589 (i) The first term is the approximation error for the original kernel matrix from
 590 the proxy point method. Then

591 (4.11)
$$\|K^{(X, Y)} - \tilde{K}^{(X, Y)}\|_F \leq \tau_1\|K^{(X, Y)}\|_F.$$

592 (ii) Next, from the SPRR factorization of $K^{(X,Z)}$,

$$593 \|K^{(X,Z)} - UK^{(\hat{X},Z)}\|_F \|\Phi^{(Z,Y)}\|_F \leq \tau_2 \|K^{(X,Z)}\|_F \|\Phi^{(Z,Y)}\|_F.$$

594 Since $\Phi^{(Z,Y)}$ is $N \times n$, (4.7) means

$$595 \|\Phi^{(Z,Y)}\|_F < \sqrt{Nn} \frac{\gamma^*}{N(\gamma_2 - \gamma^*)} = \sqrt{\frac{n}{N}} \frac{\gamma^*}{\gamma_2 - \gamma^*}.$$

596 Similarly, (4.8) and (4.9) mean

$$597 \frac{\|K^{(X,Z)}\|_F^2}{\|K^{(X,Y)}\|_F^2} < \frac{mN/(\gamma^* - \gamma_1)^{2d}}{mn/(\gamma_1 + \gamma_3)^{2d}} = \frac{N}{n} \frac{(\gamma_1 + \gamma_3)^{2d}}{(\gamma^* - \gamma_1)^{2d}}.$$

598 Then

(4.12)

$$599 \|K^{(X,Z)} - UK^{(\hat{X},Z)}\|_F \|\Phi^{(Z,Y)}\|_F < \tau_2 \sqrt{\frac{n}{N}} \frac{\gamma^*}{\gamma_2 - \gamma^*} \|K^{(X,Z)}\|_F \\ 600 < \tau_2 \frac{\gamma^*(\gamma_1 + \gamma_3)^d}{(\gamma_2 - \gamma^*)(\gamma^* - \gamma_1)^d} \|K^{(X,Y)}\|_F.$$

602 (iii) Thirdly,

$$603 \|U\|_F = \left\| P \begin{pmatrix} I \\ E \end{pmatrix} \right\|_F = \left\| \begin{pmatrix} I \\ E \end{pmatrix} \right\|_F \leq \sqrt{r + (m-r)re^2}, \\ 604 \|K^{(\hat{X},Y)} - \tilde{K}^{(\hat{X},Y)}\|_F \leq \tau_1 \|K^{(\hat{X},Y)}\|_F.$$

606 According to (4.9),

$$607 \frac{\|K^{(\hat{X},Y)}\|_F^2}{\|K^{(X,Y)}\|_F^2} = 1 - \frac{\|K^{(X \setminus \hat{X}, Y)}\|_F^2}{\|K^{(X,Y)}\|_F^2} \\ 608 \leq 1 - \frac{(m-r)n/(\gamma_1 + \gamma_3)^{2d}}{mn/(\gamma_2 - \gamma_1)^{2d}} = 1 - \frac{(m-r)(\gamma_2 - \gamma_1)^{2d}}{m(\gamma_1 + \gamma_3)^{2d}}.$$

610 Then

$$611 (4.13) \|U\|_F \|K^{(\hat{X},Y)} - \tilde{K}^{(\hat{X},Y)}\|_F \\ 612 \leq \tau_1 \sqrt{r + (m-r)re^2} \sqrt{1 - \frac{(m-r)(\gamma_2 - \gamma_1)^{2d}}{m(\gamma_1 + \gamma_3)^{2d}}} \|K^{(X,Y)}\|_F.$$

614 Combining the results (4.11)–(4.13) from the three steps above yields (4.5). To
615 show (4.6), we use the following inequality:

$$616 \|K^{(X,Y)} - UK^{(\hat{X},\hat{Y})}V^T\|_F \\ 617 \leq \|K^{(X,Y)} - \tilde{K}^{(X,Y)}\|_F + \|K^{(X,Z)}\Phi^{(Z,Y)} - UK^{(\hat{X},Z)}\Phi^{(Z,Y)}\|_F \\ 618 + \|UK^{(\hat{X},Y)} - UK^{(\hat{X},Y)}\|_F + \|UK^{(\hat{X},Y)} - UK^{(\hat{X},\hat{Y})}V^T\|_F.$$

620 Then the proof can proceed similarly. \square

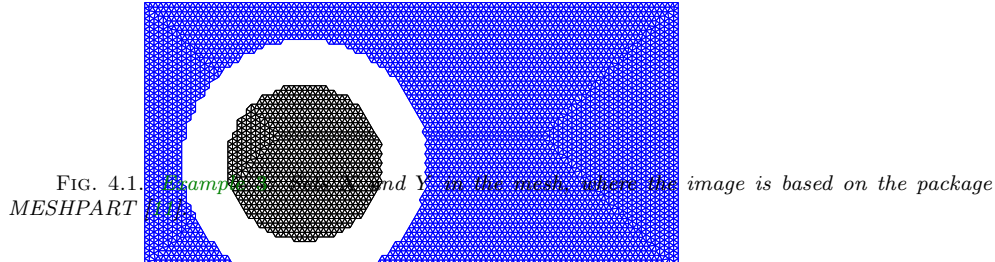
If e in SRRQR factorizations is a constant, with fixed N , the two constants in (4.5) scale roughly as $s_1 = \mathcal{O}(\sqrt{m})$ and $s_2 = \mathcal{O}(1)$. Moreover, once the annulus region $\mathcal{A}(0; \gamma_2, \gamma_3)$ is fixed, the set Y is completely irrelevant to the algorithm for obtaining the approximation (4.2) and the error bound (4.5). The column basis matrix U and the set \hat{X} of representative points can be obtained with only the set X , and the error analysis in (4.5) applies to any set Y in $\mathcal{A}(0; \gamma_2, \gamma_3)$.

Remark 4.2. Note that our error analyses in the previous section and this section are not necessarily restricted to the particular kernel like in (1.3) or the proxy point selection method. In fact, the error bounds can be easily modified for more general kernels and/or with other approximation methods as long as a relative error bound for the kernel function approximation is available. This bound is τ_1 in [Theorem 4.1](#).

We then use a comprehensive example to show the accuracies of the analytical compression and the hybrid compression, as well as the selections of the proxy points and the representative points.

EXAMPLE 3. We generate a triangular finite element mesh on a rectangle domain $[0, 2] \times [0, 1]$ based on the package MESHPART [\[11\]](#). The two sets of points X and Y are the mesh points as shown in [Figure 4.1](#), where $|X| = 821$, $|Y| = 4125$, $\gamma_1 = 0.3$, and $\gamma_2 = 0.45$. We compute the low-rank approximation in (4.2) and report the relative errors in the analytical compression step and the hybrid low-rank approximation respectively:

$$\mathcal{E}_N(\gamma) = \frac{\|K^{(X,Y)} - \tilde{K}^{(X,Y)}\|_F}{\|K^{(X,Y)}\|_F}, \quad \mathcal{R}_N(\gamma) = \frac{\|K^{(X,Y)} - UK^{(\hat{X},Y)}\|_F}{\|K^{(X,Y)}\|_F}.$$



In the first set of tests, the number of proxy points N is chosen to reach a relative tolerance $\tau_1 = 10\epsilon_{\text{mach}}$ in the proxy point method, where ϵ_{mach} is the machine precision. (Note that τ_1 is the tolerance for approximating $\kappa(x, y)$, and the actual computed Frobenius-norm matrix approximation error $\mathcal{E}_N(\gamma)$ may be slightly larger due to floating point errors.)

We vary the radius γ for the proxy surface between γ_1 and γ_2 . For $d = 1, 2, 3, 4$, $\mathcal{E}_N(\gamma)$ and $\mathcal{R}_N(\gamma)$ are shown in [Figure 4.2](#). In practice, we can use the method in [subsection 3.3](#) to obtain an approximate optimal radius $\tilde{\gamma}^*$. To show that $\tilde{\gamma}^*$ is very close to the actual optimal radius, we can look at [Figure 4.2a](#) for $d = 1$. Here, $N = 169$ and $\tilde{\gamma}^* = 0.3675$ which is very close to the actual optimal radius 0.3678 . In addition, the error bound in [Proposition 3.1](#) can be used to provide another estimate $\sqrt{\gamma_1\gamma_2} = 0.3674$. Both estimates are very close to the actual minimizer,

654 which indicates the effectiveness of the error analysis and the minimizer estimations.
 655 When $\gamma = \tilde{\gamma}^*$, we have $\mathcal{E}_N(\gamma) = 3.2106E - 16$ and $\mathcal{R}_N(\gamma) = 1.1008E - 15$, and
 656 the numerical rank resulting from the hybrid compression is 78. The numerical rank
 produced by SVD under a similar relative error is 68.

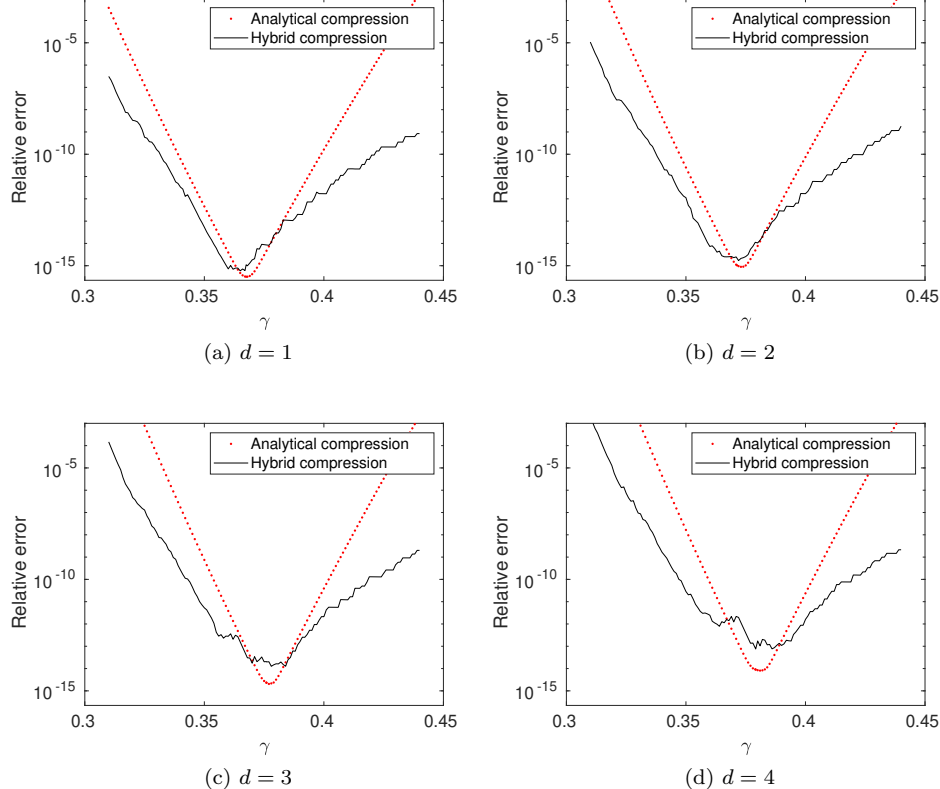


FIG. 4.2. *Example 3: $\mathcal{E}_N(\gamma)$ in the analytical compression step and $\mathcal{R}_N(\gamma)$ in the hybrid low-rank approximation with varying radius γ .*

657
 658 Similar results are obtained for $d = 2, 3, 4$. See Figure 4.2 and Table 4.1. We
 659 notice that $\mathcal{E}_N(\gamma)$ is sometimes larger than $\mathcal{R}_N(\gamma)$, especially when γ is closer to X or
 660 Y . This is likely due to the different amount of evaluations of the kernel function in
 661 the error computations. The kernel function evaluations may have higher numerical
 662 errors when γ gets closer to γ_1 or γ_2 . When γ is not too close to γ_1 or γ_2 , $\mathcal{R}_N(\gamma)$
 663 is smaller than $\mathcal{E}_N(\gamma)$, which is consistent with the theoretical estimates. Here, no
 664 stabilization is integrated into the proxy point method (which may be fixed based on
 665 a technique in [3]), while SRRQR factorizations have full stability measurements and
 666 produce column basis matrices with controlled norms. On the other hand, this also
 667 reflects that hybrid compression is a practical method.

668 Also in Figure 4.3 for $d = 1, 2$, we plot the proxy points as well as the representative
 669 points \tilde{X} produced by the hybrid approximation with $\gamma = \tilde{\gamma}^*$.

670 In our next set of tests, we vary the number of proxy points N for the analytical
 671 compression step and check its effect on the hybrid low-rank approximation error. For
 672 each N , the radius of the proxy surface γ is set to be $\tilde{\gamma}^*$. The results are shown in

TABLE 4.1

Example 3: Hybrid compression results, where $\tilde{\gamma}^*$ is the approximate optimal radius.

d	N	Optimal γ	$\tilde{\gamma}^*$	Numerical rank	$\mathcal{E}_N(\tilde{\gamma}^*)$	$\mathcal{R}_N(\tilde{\gamma}^*)$
1	169	0.3678	0.3675	78	$3.2106E - 16$	$1.1008E - 15$
2	179	0.3733	0.3713	88	$1.0431E - 15$	$2.1817E - 15$
3	187	0.3774	0.3759	93	$2.3565E - 15$	$2.0537E - 14$
4	193	0.3816	0.3792	99	$8.9381E - 15$	$7.5528E - 14$

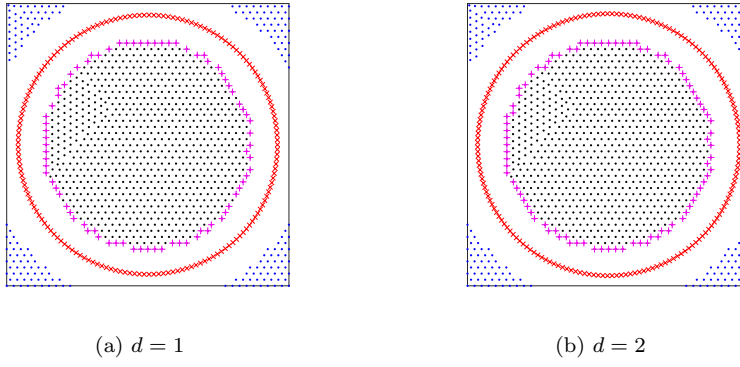


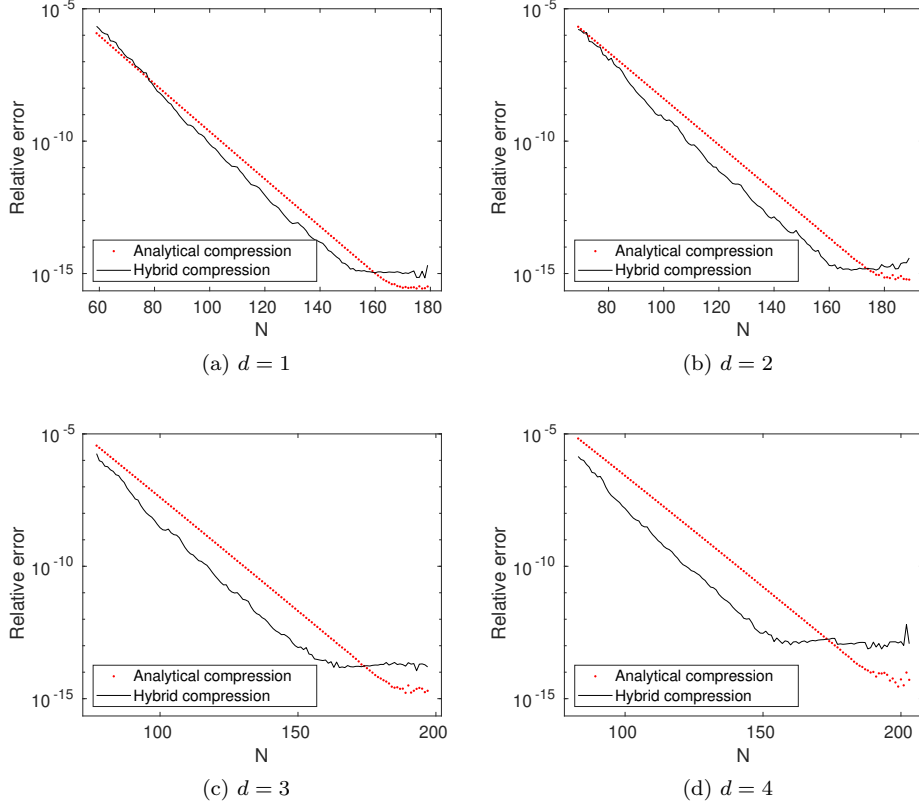
FIG. 4.3. Example 3: Representative points (+ shapes) and proxy points (x shapes).

673 **Figure 4.4.** The approximation error for the analytical compression decays exponentially as predicted by [Propositions 3.1](#) and [3.3](#) (until N reaches the values indicated 674 in [Table 4.1](#); after that point, it stops to decay due to floating point errors). 675

676 **5. Discussions.** The proxy point method has some attractive features similar 677 to some methods used for data analysis such as the Nyström method and the pseudo- 678 input approximation [\[8, 13, 26, 40, 46\]](#). For kernel matrices, both the proxy point 679 method and the Nyström method construct low-rank basis matrices directly based on 680 selections of reference points and evaluations of the original kernel function.

681 However, there are some key differences between the two methods.

682 1. The Nyström method is typically used to seek low-rank approximations for 683 *square* kernel matrices of the form $K^{(X,X)}$, which corresponds to interactions 684 within the same set X . $K^{(X,X)}$ is often heuristically considered to be of 685 low numerical rank (with modest accuracies) in data science and machine 686 learning applications. On the other hand, the proxy point method deals 687 with rectangular kernel matrices $K^{(X,Y)}$ for two different and well-separated 688 sets X and Y . If $K^{(X,X)}$ is considered, then FMM or $\mathcal{H}/\mathcal{H}^2$ /HSS matrix 689 strategies are first applied to generate well-separated subsets. That is, X is 690 first hierarchically partitioned into subsets X_i . Then the proxy point method 691 can be applied to $K^{(X_i,X_j)}$ for well-separated X_i and X_j . That is, in the 692 matrix form, the proxy point method compresses appropriate *off-diagonal* 693 *blocks* of $K^{(X,X)}$. Such an off-diagonal compression idea leads to so-called 694 rank structured matrices that have been extensively studied in the field of 695 fast solvers for some linear systems, PDEs, and integral equations. (The 696 Nyström method may also be applied to well-separated sets, but it is hard to 697 guarantee high accuracies. See the last point below.)

FIG. 4.4. *Example 3: Accuracies with $\gamma = \tilde{\gamma}^*$ and varying N .*

698
699
700
701
702
703
704
705
706
707
708
709
710
711
712
713
714
715
716
717

2. Due to the different natures of the applications that the two methods are applied to, their accuracy requirements are typically quite different. For kernel methods such as the support vector machine (SVM) or Gaussian process regression, the Nyström method produces modest accuracies (such as $\mathcal{O}(10^{-3}) \sim \mathcal{O}(10^{-1})$) which are good enough for making reasonable predictions in the model. The proxy point method considers interactions between well-separated sets instead of the entire set. For some applications, the separation of sets can be used to analytically justify the low-rankness with any specified accuracy. The proxy point method helps to conveniently compress the off-diagonal blocks of $K^{(X,X)}$ so as to quickly obtain accurate rank structured matrix approximations to $K^{(X,X)}$ that are suitable for fast and reliable direct factorizations, inversions, eigenvalue solutions, etc.
3. Since the Nyström method often select points based on techniques such as sampling and clustering, the accuracy analysis is typically probabilistic [8, 54, 55]. The proxy point method here uses a deterministic way to select proxy points. The proxy point selection and basis matrix computation are supported by analytical justifications with guaranteed controllable accuracies. The analysis enables us to rigorously quantify the error behaviors and to optimize parameters. Of course, this also means that such rigorous analysis is typically nontrivial and is feasible for specific kernels on a case-by-case basis

718 (although the method has been successfully applied to many different types of
 719 kernels in practice). Studies for many other kernels still need to be performed,
 720 and this paper serves as a starting point for such studies. In addition, as
 721 mentioned in Remark 4.2, the hybrid error analysis in Theorem 4.1 is not
 722 restricted to specific kernels or proxy point selection methods.

723 4. The Nyström method may be applied to data points in high dimensions, while
 724 the proxy point method focuses on data points in low-dimensional spaces that
 725 are often encountered in the solutions of some linear systems, eigenvalue prob-
 726 lems, PDEs, and integral equations. For example, the proxy point method
 727 are useful for direct solutions of Cauchy/Cauchy-like/Toeplitz/Vandermonde
 728 linear systems [34, 39, 49] and FMM accelerations of Hermitian eigenvalue
 729 problems [17, 45], where the data points under consideration are on some lines
 730 or curves. For some FMM techniques and PDE/integral equation solutions,
 731 the points are in one, two, or three dimensional spaces [12, 32, 33, 35, 52, 53].

732 5. The Nyström method may be extended to well-separated sets X and Y . How-
 733 ever, there is no guarantee that a specified high accuracy can be reached. For
 734 example, we may obtain an initial approximate column basis matrix $K^{(X, \hat{Y})}$
 735 by selecting a subset \hat{Y} from Y . $K^{(X, \hat{Y})}$ can be used like $K^{(X, Z)}$ in Section 4
 736 to obtain an approximation just like (4.2d). (We use this scheme so that its
 737 cost is nearly the same as our method. We may also select points from both
 738 X and Y in the Nyström method, but the accuracy in the following test is
 739 even lower.)

740 To compare the Nyström scheme in the last item above with the proxy point
 741 method for well-separated sets, we apply them to the data sets used in Example 3 by
 742 selecting the same number of points N to obtain hybrid compression. In the Nyström
 743 method, we try both random sampling with replacement and k -means clustering for
 744 selecting reference points like in [55]. The relative approximation errors for the cases
 745 $d = 1$ and 2 are plotted in Figure 5.1. The approximation accuracy from the Nyström
 746 method initially improves with increasing N , but the accuracy improvement gets very
 747 slow and almost stagnates. In comparison, the errors from the proxy point method
 748 decrease all the way to near the machine precision.

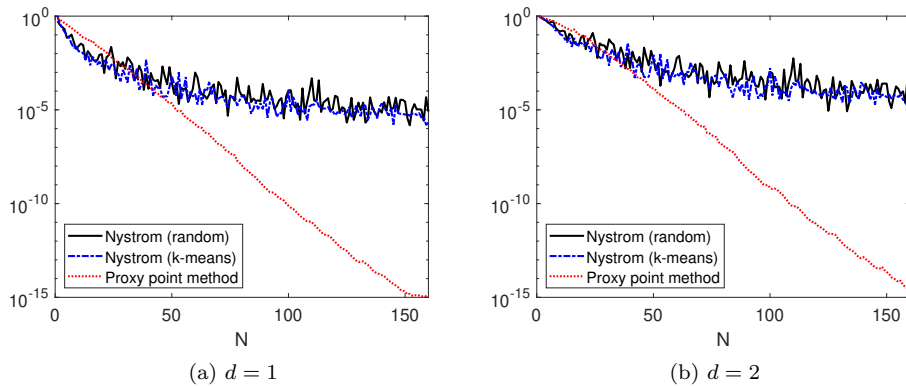


FIG. 5.1. Relative approximation errors (in Frobenius norm) of the Nyström method and the proxy point method, where the Nyström method uses random sampling or k -means clustering for selecting reference points.

6. Conclusions. The proxy point method is a very simple and convenient strategy for computing low-rank approximations for kernel matrices evaluated at well-separated sets. In this paper, we present an intuitive way of explaining the method. Moreover, we provide rigorous approximation error analysis for the kernel function approximation and low-rank kernel matrix approximation in terms of a class of important kernels. Based on the analysis, we show how to choose nearly optimal locations of the proxy points. The work can serve as a starting point to study the proxy point method for more general kernels. Some possible strategies in future work will be based on other kernel expansions or Cauchy FMM ideas [28]. Various results here are already applicable to more general kernels and other approximation methods. We also hope this work can draw more attentions from researchers in the field of matrix computations to study and utilize such an elegant method.

Acknowledgments. The authors would like to thank Steven Bell at Purdue University for some helpful discussions and thank the referees for valuable comments.

REFERENCES

[1] C. R. ANDERSON, *An implementation of the fast multipole method without multipoles*, SIAM J. Sci. Stat. Comput., 13 (1992), pp. 923–947.

[2] S. BÖRM AND W. HACKBUSCH, *Data-sparse approximation by adaptive \mathcal{H}^2 -matrices*, Computing, 69 (2002), pp. 1–35.

[3] D. CAI AND J. XIA, *Bridging the gap between the fast multipole method and fast stable structured factorizations*, preprint, 2016.

[4] R. H. CHAN, J. XIA, AND X. YE, *Fast direct solvers for linear third-order differential equations*, preprint, 2016.

[5] S. CHANDRASEKARAN, M. GU, AND T. PALS, *A fast ulv decomposition solver for hierarchically semiseparable representations*, SIAM J. Matrix Anal. Appl., 28 (2006), pp. 603–622.

[6] S. CHANDRASEKARAN, M. GU, X. SUN, J. XIA, AND J. ZHU, *A superfast algorithm for Toeplitz systems of linear equations*, SIAM J. Matrix Anal. Appl., 29 (2007), pp. 1247–1266.

[7] H. CHENG, Z. GIMBUTAS, P. G. MARTINSSON, AND V. ROKHLIN, *On the compression of low rank matrices*, SIAM J. Sci. Comput., 26 (2005), pp. 1389–1404.

[8] P. DRINEAS AND M. W. MAHONEY, *On the Nyström method for approximating a Gram matrix for improved kernel-based learning*, J. Machine Learning, 6 (2005), pp. 2153–2175.

[9] C. ECKART AND G. YOUNG, *The approximation of one matrix by another of lower rank*, Psychometrika, 1 (1936), pp. 211–218.

[10] W. FONG AND E. DARVE, *The black-box fast multipole method*, J. Comput. Phys., 228 (2009), pp. 8712–8725.

[11] J. R. GILBERT AND S.-H. TENG, *MESHPART, A Matlab Mesh Partitioning and Graph Separator Toolbox*, <http://aton.cerfacs.fr/algor/Softs/MESHPART/>.

[12] A. GILLMAN, P. M. YOUNG, AND P. G. MARTINSSON, *A direct solver with $O(N)$ complexity for integral equations on one-dimensional domains*, Front. Math. China, 7 (2009), pp. 217–247.

[13] A. GITTENS AND M. W. MAHONEY, *Revisiting the Nyström method for improved large-scale machine learning*, J. Machine Learning, 16 (2016), pp. 1–65.

[14] S. A. GOREINOV AND E. E. TYRTYSHNIKOV, *The maximal-volume concept in approximation by low-rank matrices*, Contemporary Mathematics, vol 280, 2001, pp. 47–52.

[15] L. GREENGARD AND V. ROKHLIN, *A fast algorithm for particle simulations*, J. Comput. Phys., 73 (1987), pp. 325–348.

[16] M. GU, *Subspace iteration randomization and singular value problems*, SIAM J. Sci. Comput., 37 (2015), pp. A1139–A1173.

[17] M. GU AND S. C. EISENSTAT, *A divide-and-conquer algorithm for the symmetric tridiagonal eigenproblem*, SIAM J. Matrix Anal. Appl., 16 (1995), pp. 79–92.

[18] M. GU AND S. C. EISENSTAT, *Efficient algorithms for computing a strong rank-revealing QR factorization*, SIAM J. Sci. Comput., 17 (1996), pp. 848–869.

[19] W. HACKBUSCH, *A sparse matrix arithmetic based on \mathcal{H} -matrices. Part I: Introduction to \mathcal{H} -matrices*, Computing, (1999), pp. 89–108.

[20] W. HACKBUSCH, B. KHOROMSKIJ, AND S. SAUTER, *On \mathcal{H}^2 matrices*, in *Lectures on Applied Mathematics*, Springer, Berlin, Heidelberg, 2000, pp. 9–29.

804 [21] N. HALKO, P. G. MARTINSSON, AND J. A. TROPP, *Finding structure with randomness: prob-*
 805 *abilistic algorithms for constructing approximate matrix decompositions*, SIAM Rev., 53
 806 (2011), pp. 217–288.

807 [22] K. L. HO AND L. GREENGARD, *A fast direct solver for structured linear systems by recursive*
 808 *skeletonization*, SIAM J. Sci. Comput., 34 (2012), pp. A2507–A2532.

809 [23] J. KESTYN, E. POLIZZI, AND P. T. P. TANG, *FEAST eigensolver for non-Hermitian problems*,
 810 SIAM J. Sci. Comput., 38 (2016), pp. S772–S799.

811 [24] N. KISHORE KUMAR AND J. SCHNEIDER, *Literature survey on low rank approximation of ma-*
 812 *trices*, Linear Multilinear Algebra, 65 (2017), pp. 2212–2244.

813 [25] R. KRESS, *Linear Integral Equations, Third Edition*, Springer, 2014.

814 [26] S. KUMAR, M. MOHRI, AND A. TALWALKAR, *Sampling methods for the Nyström method*, J.
 815 Machine Learning, 13 (2002), pp. 981–1006.

816 [27] X. LIU, J. XIA, AND M. V. DE HOOP, *Parallel randomized and matrix-free direct solvers for*
 817 *large structured dense linear systems*, SIAM J. Sci. Comput., 38 (2016), pp. S508–S538.

818 [28] P.-D. LÉTOURNEAU, C. CECKA, AND E. DARVE, *Cauchy fast multipole method for general*
 819 *analytic kernels*, SIAM J. Sci. Comput., 36 (2014), pp. A396–A426.

820 [29] M. W. MAHONEY AND P. DRINEAS, *CUR matrix decompositions for improved data analysis*,
 821 Proc. Natl. Acad. Sci. USA, 106 (2009), pp. 697–702.

822 [30] J. MAKINO, *Yet another fast multipole method without multipoles–pseudoparticle multipole*
 823 *method*, J. Comput. Phys., 151 (1999), pp. 910–920.

824 [31] P.-G. MARTINSSON, G. Q. ORTÍ, N. HEAVNER, AND R. VAN DE GEIJN, *Householder QR fac-*
 825 *torization with randomization for column pivoting (HQRRP)*, SIAM J. Sci. Comput., 39
 826 (2017), pp. C96–C115.

827 [32] P. G. MARTINSSON AND V. ROKHLIN, *A fast direct solver for boundary integral equations in*
 828 *two dimensions*, J. Comput. Phys., 205 (2005), pp. 1–23.

829 [33] P. G. MARTINSSON AND V. ROKHLIN, *An accelerated kernel-independent fast multipole method*
 830 *in one dimension*, SIAM J. Sci. Comput., 29 (2007), pp. 1160–1178.

831 [34] P. G. MARTINSSON, V. ROKHLIN, AND M. TYGERT, *A fast algorithm for the inversion of general*
 832 *Toeplitz matrices*, Comput. Math. Appl. 50 (2005), pp. 741–752.

833 [35] E. MICHELISSEN AND A. BOAG, *A multilevel matrix decomposition algorithm for analyzing*
 834 *scattering from large structures*, IEEE Trans. on Antennas and Propagation, 44 (1996),
 835 pp. 1086–1093.

836 [36] V. MINDEN, K. L. HO, A. DAMLE, AND L. YING, *A recursive skeletonization factorization based*
 837 *on strong admissibility*, Multiscale Model. Simul., 15 (2017), pp. 768–796.

838 [37] L. MIRANIAN AND M. GU, *Strong rank-revealing LU factorizations*, Linear Algebra Appl., 367
 839 (2003), pp. 1–16.

840 [38] M. O’NEIL AND V. ROKHLIN, *A new class of analysis-based fast transforms*. technical report,
 841 2007.

842 [39] V. Y. PAN, *Transformations of matrix structures work again*, Linear Algebra Appl., 465 (2015),
 843 pp. 107–138.

844 [40] E. SNELSON AND Z. GHAHRAMANI, *Sparse Gaussian processes using pseudo-inputs*, NIPS’05:
 845 Proceedings of the 18th International Conference on Neural Information Processing Sys-
 846 tems, (2005), pp. 1257–1264.

847 [41] E. M. STEIN AND R. SHAKARCHI, *Complex analysis*, Princeton University Press, 2003.

848 [42] X. SUN AND N. P. PITSIANIS, *A matrix version of the fast multipole method*, SIAM Rev., 43
 849 (2001), pp. 289–300.

850 [43] L. N. TREFETHEN AND J. A. C. WEIDEMAN, *The exponentially convergent trapezoidal rule*,
 851 SIAM Rev., 56 (2014), pp. 385–458.

852 [44] E. E. TYRTYSHNIKOV, *Mosaic-skeleton approximations*, Calcolo, 33 (1996), pp. 47–57.

853 [45] J. VOGEL, J. XIA, S. CAULEY, AND V. BALAKRISHNAN, *Superfast divide-and-conquer method*
 854 *and perturbation analysis for structured eigenvalue solutions*, SIAM J. Sci. Comput., 38
 855 (2016), pp. A1358–A1382.

856 [46] C. WILLIAMS AND M. SEEGER, *Using the Nyström method to speed up kernel machines*, Ad-
 857 *vances in Neural Information Processing Systems 13*, (2001), pp. 682–688.

858 [47] J. XIA, *Randomized sparse direct solvers*, SIAM J. Matrix Anal. Appl., 34 (2013), pp. 197–227.

859 [48] J. XIA, S. CHANDRASEKARAN, M. GU, AND X. S. LI, *Fast algorithms for hierarchically semisep-
 860 arable matrices*, Numer. Linear Algebra Appl., 17 (2010), pp. 953–976.

861 [49] J. XIA, Y. XI, AND M. GU, *A superfast structured solver for Toeplitz linear systems via ran-*
 862 *domized sampling*, SIAM J. Matrix Anal. Appl., 33 (2012), pp. 837–858.

863 [50] X. XING AND E. CHOW, *An efficient method for block low-rank approximations for kernel*
 864 *matrix systems*. preprint, 2018.

865 [51] X. YE, J. XIA, R. H. CHAN, S. CAULEY, AND V. BALAKRISHNAN, *A fast contour-integral*

866 *eigensolver for non-hermitian matrices*, SIAM J. Matrix Anal. Appl., 38 (2017), pp. 1268–
867 1297.

868 [52] L. YING, *A kernel independent fast multipole algorithm for radial basis functions*, J. Comput.
869 Phys., 213 (2006), pp. 451–457.

870 [53] L. YING, G. BIROS, AND D. ZORIN, *A kernel-independent adaptive fast multipole algorithm in
871 two and three dimensions*, J. Comput. Phys., 196 (2004), pp. 591–626.

872 [54] K. ZHANG AND J. T. KWOK, *Block-quantized kernel matrix for fast spectral embedding*, Pro-
873 ceedings of the 23rd international conference on Machine learning, (2006), pp. 1097–1104.

874 [55] K. ZHANG, I. W. TSANG, AND J. T. KWOK, *Improved Nyström low-rank approximation and er-
875 ror analysis*, Proceedings of the 25th international conference on Machine learning, (2008),
876 pp. 1232–1239.